INDUCTION OF MYELOID-DERIVED SUPPRESSOR CELLS BY UVEAL MELANOMA CELL LINES

Cristina Fonseca | 260804308

MUHC-McGill Ocular Pathology & Translational Research Laboratory

Department of Pathology

McGill University, Montreal

August 2020

Thesis submitted to the Graduate Studies Program at McGill University in partial fulfillment of the requirements of the degree of Master of Science.

TABLE OF CONTENTS

ABSTRACT

Uveal melanoma (UM) is the most common primary intraocular tumor in adults and has a high mortality rate due to metastatic disease. Metastasis development is enabled by a tumor-induced immunosuppressive environment. Myeloid-derived Suppressor Cells (MDSCs), a heterogeneous population of immature myeloid cells, which can mediate suppression of T-effector responses, have been recently implicated in cancer immunotolerance and failure of anti-tumor activity. Human MDSCs are characterized based on their phenotypic features by displaying myeloid markers and further subcategorized into early-stage, granulocytic or monocytic subsets. Herein, this study aims to evaluate *in vitro* interactions between MDSCs and UM cells, especially the ability of primary and metastatic UM cell lines to induce expansion of MDSCs from peripheral blood mononuclear cells (PBMCs), and compare them in terms of phenotype and suppressive function. Secondary aims include evaluation of different concentrations of Celecoxib (selective COX-2 inhibitor) on induced myeloid cells and characterization of supernatants from PBMCs/ UM co-cultures, in terms of released cytokines/ growth factors.

A defined methodology for in vitro induction of $CD11b^{+}CD33^{+}$ myeloid cells was developed based on co-cultures of PBMCs with tumor cells, preventing cell-to-cell interaction. The analysis of supernatants showed significant differences in the concentration of several growth factors and inflammatory cytokines such as GM-CSF, IFN-γ, IL-1β, IL-6, IL-10 and TNF-α, when comparing co-cultures of PBMCs with tumor cells and without tumor cells. Myeloid cells, isolated from co-cultures with UM cell lines MEL270, OMM2.5 and 92.1, displayed phenotypic markers of human MDSCs, and exhibited suppressive properties on autologous T-cell proliferation. Different tumor cell lines demonstrated the ability to induce suppressive MDSCs, with different suppressive potencies, in comparison to myeloid cells cultured in the

absence of tumor cells. Furthermore, the addition of Celecoxib was not effective in rescuing T-cell proliferation among the cell lines tested.

This study revealed that UM cell lines have the ability to induce MDSCs with different suppressive potencies, through soluble factors, in a relatively short period of time. Our work contributes to better understand the role of MDSCs in tumor-related immunossupression, and may pave the way for the development of adjuvant therapies targeting MDSCs, ultimately contributing to improve UM patients' survival.

RESUMÉ

Le mélanome uvéal (MU) est la tumeur intraoculaire primaire la plus fréquente chez les adultes, avec un taux de mortalité élevé dû à la dissémination métastatique. Le développement des métastases est facilité par un environnement immunosuppresseur induit par la tumeur. Les cellules suppressives dérivées de myéloïdes (CSDM), une population hétérogène de cellules myéloïdes immatures qui ont un rôle dans les réponses des cellules effecteurs T et qui ont été récemment impliquées dans l'immunotolérance au cancer et l'échec de l'activité anti-tumorale. Les CSDM humaines sont caractérisées en fonction de leurs marqueurs phénotypiques et sous catégorisées en CSDM de stade précoce, granulocytaires ou monocytaires. Cette étude vise à évaluer les interactions *in vitro* entre les CSDM et les cellules MU; en particulier la capacité des lignées cellulaires de UM primaires et métastatiques à induire l'expansion des CSDM à partir de cellules mononuclées du sang périphérique (CMSP), et comparer leur phénotype et leur fonction suppressive. Les objectifs secondaires incluent l'évaluation de différentes concentrations de Célécoxib (inhibiteur sélectif de la COX-2) sur les cellules myéloïdes induites et la caractérisation des surnageants des co-cultures CMSP/ MU, en termes de cytokines et facteurs de croissance libérés.

Nous avons développé une méthodologie définie pour la génération in vitro de cellules myéloïdes $CD11b^{+}CD33^{+}$ en utilisant des co-cultures de CMSP avec des cellules tumorales, empêchant l'interaction cellule à cellule. L'analyse des surnageants a montré des différences importantes dans la concentration de plusieurs facteurs de croissance et cytokines inflammatoires, tels que GM-CSF, IFN-γ, IL-1β, IL-6, IL-10 et TNF-α, entre les co-cultures de CMSP avec et sans les cellules tumorales. Les cellules myéloïdes, isolées à partir de co-cultures avec les lignées cellulaires UM MEL270, OMM2.5 et 92.1, présentaient des marqueurs phénotypiques de CSDM humains et des propriétés suppressives sur la prolifération des

lymphocytes-T autologues. Différentes lignées cellulaires tumorales ont démontré la capacité d'induire des CSDM suppressives, avec des puissances suppressives différentes, en comparaison avec des cellules myéloïdes cultivées dans l'absence de cellules tumorales. De plus, l'ajout du Célécoxib n'a pas été efficace pour préserver la prolifération des lymphocytes-T parmi les lignées cellulaires testées.

Cette étude révèle que les lignées cellulaires MU ont la capacité d'induire des CSDM avec différentes puissances suppressives, grâce à des facteurs solubles, dans un espace de temps relativement court. Nos travaux contribuent à mieux comprendre le rôle des CSDM dans l'immunosuppression liée aux tumeurs, et peuvent ouvrir chemin au développement de thérapies adjuvantes ciblant les CSDM, ce qui pourrait contribuer à améliorer la survie des patients avec le MU.

ACKNOWLEDGMENTS

This thesis is the result of a life changing challenge I embraced on January 2019: translational research. I put a hold on my career as an ophthalmologist and travelled to Canada to start a Master's Program in Pathology, at the renowned McGill University. This exciting adventure was only possible thanks to the amazing support of my supervisor, Dr. Miguel Burnier, who has believed in me since the day we first met. Joining Dr. Burnier's Laboratory opened a new world of possibilities and gave me the privilege to learn and work with a team of inspiring and dedicated researchers, who I now call my friends. Many thanks are also in order to my thesis advisors, Dr. Jean Deschenes and Dr. Hady Saheb for their time and opinions, that ultimately improved my project.

I would like to thank Dr. Edith Zorychta and Dr. Hua Ling for their amazing work at the Pathology Department, their passion for teaching and their genuine kindness, welcoming so many different people, making them feel at home.

A word of gratitude is due to colleagues and friends, members of the Lab and the Research Institute, who welcomed me and generously shared their time and knowledge with me, greatly contributing to this project, especially Ekaterina Yurchenko, Ana Beatriz Dias, Tiffany Porracio and Thupten Tsering. A very special thanks to my friends, my "around the world-Canadian family" Alex Laskaris, Alicia Goyeneche, Christina Mastromonaco, Myriam McDonald, Paulina Garcia de Alba, Rita Proença and Tadhg Ferrier, who made this adventure into an amazing and enriching life experience.

I would like to dedicate this work to the memory of a great friend, Dr. Júlia Fernandes, who always encouraged me to go further and never stopped believing in me. Finally, I'd like to thank my parents, my sister, Magui and Diogo, my family and my close friends for their support and daily presence, even with an ocean's distance between us. Their presence,

support and love was always felt, throughout all the good and less good moments, urging me to pursue my goals and never give up. My last word of gratitude goes to Henrique, for being my life partner and my ultimate supporter, in all my life projects and adventures.

CONTRIBUTION OF AUTHORS

This is to certify that the candidate has conceived this research project and developed a methodology to answer the proposed research questions. The experiments described in this thesis were conducted by the student, under the supervision of Dr. Miguel Burnier and the bright guidance of Dr. Alicia Goyeneche and Dr. Ekaterina Yurchenko. Flow cytometry live cell sorting was performed by Dr. Ekaterina Yurchenko from the Research Institute Immunophenotyping Core. Supernatant analysis using Luminex™ 200 system was performed by Eve Technologies Corporation (Calgary, Alberta).

A manuscript originating from this thesis is under preparation for submission.

LIST OF ABBREVIATIONS

AC	Anterior chamber
ACAID	Anterior-chamber associated immune deviation
aCGH	Array Comparative Genomic Hybridization
ADAM17	ADAM metallopeptidase domain 17
AJCC	American Joint Comission on Cancer
ARG-1	Arginase-1
BAP-1	BRCA-1 associated protein
BCL-XL	B-cell lymphoma XL
CCL2	Chemokine (C-C motif) ligand 2
CFSE	Carboxyfluorescein diacetate succinimidyl ester
CM	Conditioned medium
CNV	Copy number variations
COMS	Collaborative Ocular Melanoma Study
COX-2	Cyclooxygenase-2
CTC	Circulating tumor cell
CTL	Cytotoxic T-lymphocytes
CTLA-4	Cytotoxic T-lymphocyte-associated protein 4
CXB	Celecoxib
CXCR	C-X-C motif chemokine receptor
C/ERPB	CCAAT/enhancer-binding protein-B
DC	Dendritic cell
DMSO	Dymethyl sulfoxide
DNA	Deoxyribonucleic acid
EBT	Episcleral Brachytherapy
FACS	Fluorescence-activated cell sorting
FBS	Fetal bovine serum
FISH	Fluorescence in-situ hybridization
FMO	Fluorescence minus one
FS/SC	Forward scatter/ side scatter
GEP	Gene expression profiling

G	Granulocyte
GM-CSF	Granulocyte-macrophage colony-stimulating factor
HIF-1α	Hypoxia inducible factor-1α
ICI	Immune checkpoint inhibitor
IDO-1	Indoleamine 2,3-deoxygenase
IFN	Interferon
IL	Interleukin
(i)NOS	Inducible nitric oxyde synthase
JAK	Janus kinase
LOX-1	Lectin-type oxidized LDL receptor-1
M	Monocytic
M3	Monosomy 3
MAPK	MAP kinase
MCM	Melanoma conditioned medium
MDSC	Myeloid-derived Suppressor Cell
MFI	Mean intensity fluorescence
MHC	Major Histocompatibility Complex
MIF	Migration inhibitory factor
MLPA	Multiplex ligation-dependent probe amplification
miRNA	MicroRNA
MMP	matrix metalloproteinase
mRNA	Messenger RNA
NADPH	Nicotinamide adenine dinucleotide phosphate
NF- κB	Nuclear factor kappa-light-chain-enhancer of activated B-cells
NK	natural killer
NO	Nitric Oxyde
PBMC	Peripheral blood mononuclear cells
PBS	Phosphate buffered saline
PD-1/PD-L1	Programmed death 1/ programmed death-ligand 1
PDT	Photodynamic Therapy
PGE_2	Prostaglandin E_2
PMN	Polymorphonuclear

PNT	Peroxynitrite
PRAME	Preferentially expressed antigen in melanoma
rh	Recombinant human
RNA	Ribonucleic acid
RNS	Reactive nitrogen species
ROS	Reactive oxygen species
RPMI	Roswell Park Memorial Institute
ScRNA	Single-cell RNA
STAT	Signal transducer and activator transcription
TAM	Tumor-infiltrating macrophages
TCR	T-Cell Receptor
TGCA	The Cancer Genome Atlas
TFME	Tumor-free microenvironment
TGF-β	Transforming growth factor-β
Th	Thelper
TIL	Tumor-infiltrating lymphocytes
TME	Tumour microenvironment
Tregs	Regulatory T-cells
TXA_2	Thromboxane A2
UM	Uveal Melanoma
UV	Ultraviolet
VEGF	Vascular endothelial growth factor

LIST OF FIGURES AND TABLES

1. INTRODUCTION

1.1. Uveal Melanoma

1.1.1. Epidemiology

Uveal melanoma (UM) is the most common primary intraocular tumor in adulthood and accounts for about 3-5% of all melanomas [1,2]. The incidence varies with sex, age, race and latitude [1]. In Europe, standardized incidence rates diverge from less than 2 cases per million in Southern countries such as Spain and Italy, to 4-6 per million in Central Europe, up to more than 8 per million in Northern Countries like Sweden and Denmark [3]. In the United States (US), the mean age-ajusted incidence of UM was 5.1 per million from 1973 to 2008 [4]. In Canada, a recently published population-based study reported an average annual incidence rate of 3.75 cases per million [5]. A south-to-north increasing incidence gradient is apparent and may be related to the higher degree of ocular pigmentation in southern populations, with consequent protection against ultraviolet (UV) radiation [2,6]. Correspondingly, UM is more common in the White population, compared to Black, Hispanic or Asian races [2]. According to US studies, more than 95% of patients were White, with a Black:White incidence ratio of 196:1 [4]. In Asians, the incidence is approximately 0.38 per million, per year [7].

Uveal melanoma most commonly affects older age groups, with a mean age of presentation around 60 years [2,6]. In Canada, the mean age of UM diagnosis was 61.5 ± 14.21 years and age distribution analysis showed that almost 60% of UM patients from 1992-2001 were older than 60 years [5]. Similarly, in the US, median age at diagnosis was 62 years-old, showing increase since 1973 (59 years-old) [4,8].

Some factors have been reported as predisposing to UM, including host factors and external factors [2,5]. Host factors include light and fair hair/skin complexion and light coloured irises, oculodermal melanocytosis, family history of uveal melanoma, germline

mutations in BRCA-1 associated protein (BAP1) and familial dysplastic nevus syndrome. Environmental (external) factors as blue and ultraviolet (UV) light exposure are still arguable, and while this association is consistent for UV and cutaneous melanoma, it is not for UM [2,5,6].

1.1.2. Clinical Presentation

Uveal melanomas include tumors arising from choroidal melanocytes in more than 90% of cases, but they can also develop from the ciliary body or the iris [2]. Clinically, small choroidal melanomas are slightly elevated lesions and, as they grow and break throught the Bruch's membrane, they present as dome-shaped or mushroom-configured masses [2,6]. When tumors infiltrate through the retina, vitreous hemorrhage can occur [6,9]. Rarely (around 3% of UM), can present as diffusely infiltrative into the choroid, without forming elevated masses [9,10]. Patients presentation depends on the location and dimension of the tumor. Most lesions located in the posterior pole present with painless visual loss, associated with serous retinal detachment [9]. Photopsia, floaters, visual field loss or pain can also be presenting symptoms, or sometimes the patient is asymptomatic [2,6]. UM can vary in pigmentation, from heavily pigmented to totally amelanotic [2,9].

Ciliary body melanomas, due to their location behind the iris, are diagnosed later than iris or choroidal melanomas, presenting as fairly large masses, deforming the iris and angle, and causing rapidly progressive cataracts [2,9]. Iris melanomas are more readily apparent enlarging masses and, although much less common (3-5% of all uveal melanomas) [11], are usually diagnosed much earlier than ciliary body or choroidal melanomas [2].

1.1.3. Pathology

UM arises from melanocytes in the uveal stroma. These tumors are composed of malignant melanocytes that can be classified according to their morphology into spindle cells and epithelioid cells [9,12,13]. These cells can be pigmented or non-pigmented. Spindle shaped cells have fusiform shape and grow in a syncytial form, forming interweaving fascicles of parallel oriented cells and can be classified in type A or B, according to their nuclear characteristics [9,12]. Spindle type A cells have elongated nuclei, with fine chromatin, indistinct nucleolus, and often the nuclear membrane has a characteristic longitudinal striation. Spindle-type B cells have a bulkier nucleus, with coarse chromatin and prominent nucleoli and eosinophilic nuclei [9,12]. Epithelioid cells are larger, polygonal, more pleomorphic and have abundant cytoplasm. They have large, rounded nuclei with coarse chromatin and large and eosinophilic nucleoli [9,12].

UMs are cytologically classified in three categories: spindle cell melanomas (UMs composed of malignant spindle cells A and B); mixed cell type UMs (contain either spindle cells and epithelioid cells); and epithelioid UMs (composed predominantly of epithelioid cells and relatively rare). Most medium and large sized-UM are mixed cell type UM [9,12].

1.1.4. Treatment and Prognosis

Enucleation was the treatment of choice for uveal melanomas until the mid-20th century. After the 70s, the controversy about the negative effects of enucleation described in the "*Zimmerman Hypothesis*" allowed the development of other therapeutic alternatives, especially globe-sparing approaches [14]. In 1985, the National Eye Institute funded a multicentric randomized clinical trial with three arms, aiming to compare the outcomes of different therapies for large and medium choroidal melanomas, and evaluate the natural

history of small choroidal UM [15]. The Collaborative Ocular Melanoma Study (COMS) contributed to establishing the pivotal role of episcleral brachytherapy (EBT) in the treatment of medium and some large melanomas, thus becoming the most common globe-preserving treatment for uveal melanoma in the world [14,15]. Other conservative treatments for UM can be performed on small size tumors located in the posterior pole and include laser photocoagulation, photodynamic therapy (PDT) and transpupillary thermotherapy [2,14].

In the COMS study, patients with medium-sized choroidal melanomas were randomized to undergo either enucleation or ^{125}I brachytherapy. Survival data showed no differences in mortality between patients assigned to either form of treatment [15,16]. Despite great local control rates, the all-cause 12-year mortality rate was around 40%, regardless of the therapeutic modality used for treatment [16]. Mortality following histopathologically confirmed melanoma metastasis was 21% in the ^{125}I brachytherapy group and 17% in the enucleation group [16].

The main clinical challenge of UM is its high tendency to metastize and associated high mortality rate. Outcomes are exceedingly poor following the development of metastatic disease. Approximately 20–30% of patients diagnosed with primary uveal melanoma die of systemic metastasis within 5 years of diagnosis, and 45% die within 15 years [17,18].

Due to the lack of lymphatic drainage of the eye and orbit, UM spreads hematogenously and most of the patients develop liver metastasis, which are fatal in a short period of time [6,9]. Therefore, there has been an effort to determine prognostic factors that can identify patients at higher risk to develop metastatic disease. The importance of an accurate prognostic information is vital for the selection of individualized screening and treatment plans.

Prognostic factors include clinical features as size of the tumor, involvement of the ciliary body and the presence of extraocular extension [1,2,9]. In fact, these three clinical factors are used to classify the tumours according to the *American Joint Comission on Cancer* (AJCC), which has a prognostic value [19]. In addition to clinical features, prognostic factors are also evident in histolopathological examination as: epithelioid cell type within the tumour, vascular mimicry (microvascular closed loops), mitotic activity, and tumor-infiltrating lymphocytes (TILs) and macrophages [9,20].

However, genetic alterations have become increasingly important to estimate prognosis and current tests rely on either DNA or RNA extraction from tumor specimens. Genetic poor prognosis predictors include chromosome 3 loss (partial or total), chromosome 6 loss, chromosome 8q gain or 8p loss, chromosome 1p loss and *BAP-1* gene loss [2,11]. Techniques as *fluorescence in-situ hybridization* (FISH), *multiplex ligation-dependent probe amplification* (MLPA), *array comparative genomic hybridization* (aCGH) and karyotyping are commonly used for DNA analysis; gene expression profiling (GEP) is the preferred technique for RNA-based prognostication [21]. The prognostic value of the standard 15-gene assay in GEP has been validated in a multicentric clinical trial, and patients having UM categorized as GEP class 2 present a much higher risk of metastatic disease than patients in GEP class 1 [22]. However, mRNA expression of the cancer-testis antigen, preferentially expressed antigen in melanoma (PRAME) was associated with shorter time to melanoma-specific mortality for both Class 1 and Class 2 UM tumors [18]. Since PRAME has been successfully targeted for immunotherapy, it may prove to be an additional prognostic biomarker with a superior prognostic accuracy for Class 1 disease. The 5-year metastatic risk for patients with Class 1a, 1b and 2 uveal melanomas are 2%, 21% and 72%, respectively [9,18].

More recently, the Cancer Genome Atlas Project (TGCA) analyzed data from 80 UM specimens, regarding mutations, genomic copy number alterations, transcriptomic and methylation profiles [23,24]. This study allowed the definition of four molecular and clinical subsets in UM: two associated with poor prognosis and monosomy 3 and two associated with better prognosis and disomy 3/ chromosome 6p gain [23,24].

Nonetheless, although prognostication in UM has achieved high precision, some limitations cannot be ignored, the most relevant being spatial and temporal tumor heterogeneity that cannot be totally captured with a single-time tissue biopsy.

1.1.5. Metastatic Uveal Melanoma

The advances treating UM primary tumor do not reflect on survival rates. Metastatic disease occurs predominantly in the liver (80% of cases) and is associated with poor survival (median 4-15 months) [25].

Metastatic UM treatment is currently limited by the lack of effective systemic therapy options. The intrinsic resistance of UM to conventional systemic chemotherapy has led researchers to search for new approaches [18]. Molecular biology and a better knowledge of cancer cells genetics has allowed the development of new therapeutic targets. Various treatments have been evaluated, including systemic chemotherapy, immunotherapy, targeted agents against the MAPK pathway, and liver-directed therapies, but response rates are generally less than 10% and, more importantly, no therapy has improved overall survival [18].

Immunotherapy is currently an exciting area of drug development for cancer, carrying the prospect of durable remissions and even cure for metastatic disease. In patients with advanced cutaneous melanoma, immunotherapy has dramatically improved survival

outcomes [18]. Immune checkpoints are regulatory pathways that play a key role on adaptive immune responses. They provide natural counterbalance to immune activation, functioning as breaking signals for the immune response, and as checkpoints that effector T-cells must pass to exert their functions.

Unfortunately, although widely used, established agents against immune checkpoints CTLA-4 and PD-1/PD-L1 have been disappointing in UM [18,26]. Response rates to single-agent therapies are around 5% and combinations of immune checkpoint inhibitors (ICIs) were also unable to provide benefit for patients with metastatic UM [26,27].

The difference in ICIs efficacy between UM and cutaneous melanoma is partly related to differences in mutational load and cancer immunogenicity [18,23,26]. The greater the number of mutations in a tumor, the more probable that some of those mutations will provide the expression of neoantigens, providing targets for T-cells [28]. Highly immunogenic cancer cells are more prone to be eliminated by immunocompetent hosts (immunoediting); less immunogenic clones are less probable to stimulate an immune response, allowing them to grow and proliferate [29]. A recent study by TGCA showed markedly lower somatic mutation rates in UM in comparison to cutaneous melanoma, or other cancer types [23,30].

1.2. Immune Response in Cancer

In 2000, Hanahan and Weinberg defined the six hallmarks of cancer as abilities that enable tumor growth and the metastatic process, and include: sustained proliferative signaling, growth suppression resistance, cell death resistance, limitless growth potential, sustained angiogenesis and metastatic potential [31,32]. A decade later, these authors added two emerging hallmarks to the list: reprogrammation of cell energy metabolism and eviction of immune destruction [29].

In the metastatic cascade, intravasation of tumor cells into the circulation is essential, but it represents only one of the multiple steps needed. For formation of metastasis, malignant cells must be able to acquire specific genotypic and phenotypic features, escape immune control, leave the bloodstream, establish themselves in a new microenvironment and colonize distant organs. The success rate of metastasis is low, only a small percentage of the released circulating tumor cells (CTCs) will persist and form secondary lesions [29]. Apart from surviving mechanical stress in the bloodstream, these cells must also be prepared to interact with the host immune system. Likewise, colonization of distant organs does not always translate into metastatic disease, as evidenced by the presence of micrometastasis in many patients that never progress into macroscopic tumors [29].

The theory of immunosurveillance proposes that the immune system can recognize and eliminate the majority of incipient cancer cells, keep micrometastasis controlled and mantain tumor cells dormant [33,34]. Innate and adaptive immunity act as complementary networks of self-defense against foreign threats, including pathogens and cancer. The innate immune response is the body's first line of defense, as it is rapid and antigen-independent, as includes cell populations like granulocytes (neutrophils, eosinophils, basophils and mast cells), monocytes/macrophages and dendritic cells. In contrast, adaptive immune response is antigen-specific and able to produce a durable response. Although not immediate, once activated, it can be sustained through an immune memory response. Cytotoxic T lymphocytes (CTLs) are the main effector cells of the adaptive immune system [28].

Both the innate and adaptive immune responses have the potential to recognize and eliminate abnormal cells, such as tumor cells. However, those can evolve at any phase of their growth to outsmart the antitumor immune response, evade or suppress the host's natural

response. The generation of anti-cancer immune response is a cyclic process (the Cancer-Immunity Cycle), a series of steps that lead to the accumulation of stimulatory factors and amplification of T-cell responses [28]. The cycle is also characterized by the presence of inhibitory feedbacks and mechanisms that regulate the immune response [28]. In cancer, this cycle may fail during any of the steps: no detection of tumor antigens, no recognition of tumor antigens as *non-self*, inability to infiltrate the tumours or suppression of effector T-cell responses. The immune profile of a patient is determined by a multitude of intrinsic and extrinsic factors, which determine the "cancer-immune set point", the equilibrium between the promotion and suppression of anticancer immunity [28].

Tumor progression and metastatic disease development can be enabled by an immunosuppressive environment [33,35]. This is particularly striking when analyzing the epidemiological data regarding prevalence of certain types of tumours in immunossupressed patients; and also verified in genetically modified immunodeficient mice models, particularly defective in $CD8^+$ cytotoxic T-cells, $CD4^+$ Th_1 (T-helper) cells and natural killer (NK) cells, which are more susceptible to developing malignancies. These results show a major role of the immune system in cancer survaillance [29,36,37].

1.2.1. Immune Response in Uveal Melanoma

The eye has long been considered an immune priviledged site, protecting ocular tissues and vision from inflammatory damage [30,38,39,40]. This is achieved by structural barriers (separating the blood from intraocular compartments), ocular resident cells, soluble suppressive factors as transforming growth factor (TGF)-β and macrophage migration inhibitory factor (MIF), and a phenomenon known as anterior-chamber associated immune deviation (ACAID) [30,40,41]. Arising from this immunopriviledged environment, UM cells

retain some escape mechanisms that allow them to elude the immune system and facilitate systemic dissemination.

Similarly to other tumours, primary UM cells interact with both innate and adaptive immune populations. The immune infiltrate in UM is associated with a poorer prognosis [9,20] and is composed of several different populations, consisting of $CD8^+$ T-lymphocytes, some $CD4^+$ T-lymphocytes, Foxp3 regulatory T-cells (Tregs) and $CD68^+CD163^+$ M2 macrophages [38,39,41]. Tregs are a specialized suppressive T-cell subpopulation and their frequency in primary UM has been correlated with metastatic disease [38,39,40,41]. Furthermore, tumor-associated macrophages (TAMs) are predominantly polarized towards a suppressive M2 phenotype, capable of secreting anti-inflammatory cytokines (IL-10 and TGF-β) and inhibiting dendritic cell activation and T-/NK-cell function [38,39,41]. M2-macrophages are also responsible for promoting angiogenesis and enhancing tumor cells invasive abilities [38,39,41]. Inside this complex microenvironment, UM have adapted to exploit local host immune response in order to survive and disseminate.

Additionally, the Cancer Genome Atlas (TCGA) Project showed that poor prognosis monosomy 3 (M3) UM subsets showed distinct genomic and immune profiles. MicroRNA (miRNA) sequencing analysis identified four UM clusters, which were clearly associated with M3. miRNA cluster 4 corresponded to M3 UM with immune infiltration, suggesting that expression of certain miRNA might be associated with promotion of an immune environment, that plays a significant role in aggressive UM [23]. As previously recognized, the interplay between tumor cells, immune cells and soluble factors promotes tumor growth and dissemination [38,39].

It is a common belief that metastatic disease is not a late stage occurrence in the natural history of UM. It has been proven that the presence of micrometastasis occurs early in the

progression of the disease [33]. In fact, Eskelin et al and Singh estimated the time of micrometastasis in UM to develop to be 2.9 years earlier than the diagnosis of the primary tumor, indicating that dissemination has occurred before conservative treatment of the primary malignancy [42,43]. Callejo and colleagues showed that CTCs can be detected from the diagnosis until later stages of the disease, independently of tumor size [44].

Circulating tumor cells interact with a myriad of immune cell populations in the bloodstream [33,35]. There are immune cell populations that act to eliminate the tumor, whereas paradoxically others have a pro-tumorigenic effect [33,35]. This immunological pressure may induce mechanisms that enable tumor cells to evade immune recognition and/or actively suppress the immune response. Cancer cells can directly disable effector immune cells as cytotoxic T-cells or NK cells, or indirectly skew T-cell responses from a Th1 subset to the Th2 phenotype or induce inflammatory cells that have immunossupressive properties, including Tregs and Myeloid-derived Suppressor Cells (MDSCs).

The mechanisms regulating UM immune escape remain elusive and are most probably responsible for its progressive course, poor prognosis and treatment resistance (low efficacy of ICIs [18,24]. One proposed mechanism for UM immune evasion is through the induction of MDSCs. McKenna KC *et al* showed that the injection of thymoma tumor cells in the skin and anterior chamber (AC) of immunocompetent mice originated antigen-specific $CD8^+$ CTL infiltration that eliminated the skin tumor but not the primary ocular tumor, demonstrating that ocular immune priviledge may interfere with CTL lytic activity [45]. These authors further demonstrated the infiltration of primary ocular tumours by $CD11b^+$ cells, which were capable of suppressing CTL responses *in vitro*. Based on their observations, the authors hypothethized that local $CD11b^+$ myeloid suppressor cells would inhibit the CTL responses, allowing the tumors to grow [45].

1.3. Myeloid-Derived Suppressor Cells (MDSC)

Myeloid cells are a diverse population that arise from myeloid progenitor cells during hematopoiesis and generate terminally differentiated mononuclear and granulocytic cells. The first include monocytes, which differentiate in tissues to macrophages and dendritic cells (DCs); the latter terminally differentiated populations include polimorphonuclear neutrophils, eosinophils, basophils and mast cells [46]. During an acute inflammatory stimuli, emergency myelopoiesis is activated in the bone marrow to increase the pool of phagocytic cells and the release of pro-inflammatory cytokines, terminating upon cessation of the insult [46,47,48]. However, in cases of chronic inflammation or cancer, persistent low-strength signals stimulate aberrant sustained myelopoiesis, characterized by the accumulation of immature, undifferentiated myeloid cells in the bone marrow, peripheral tissues, bloodstream and lymph nodes [46,47,48]. These immature granulocytic and monocytic myeloid cells, although phenotypically similar to the mature, differentiated counterparts show, not only different genomic and biochemical profiles, but also distinct functional activity, namely the ability to supress antigen-specific and antigen non-specific T-cell responses [46,47,49,50].

The first report regarding accumulation of myeloid cells capable of inhibiting CTLs was described in the late 1970s, followed by the description of $CD11b^{+}Gr\text{-}1^{+}$ myeloid cells in tumour bearing mice in the late 1990s, with potent immunossuppressive properties. However, with growing research on these cells, it soon become clear they were a highly heterogeneous population, rendering the need for an unified description. In 2007, the name myeloid-derived suppressor cells (MDSCs) was proposed, considering their myeloid origin and heterogeneity, their immunossuppressive functions and their expansion in a cancer-dependent setting [46,47,49].

1.3.1. Phenotypic Characterization

Two major subpopulations of MDSCs can be distinguished based on their morphological and phenotypic features: polymorphonuclear (PMN) and monocytic (M)-MDSCs (51). In mice, these subpopulations were identified by the expression of lymphocyte antigens Ly-6C and Ly-6G [46,47,49]. The M-MDSC subpopulation has a monocytic-like appearance and preferentially express $CD11b^{+}Ly\text{-}6G^{low}$ $Ly\text{-}6C^{hi}$; the PMN-MDSC subpopulation shows a polymorphonuclear morphology and is characterized by the markers CD11b+ $Ly\text{-}6G^{hi}$ $Ly\text{-}6C^{low}$ [49,51]. In humans, the phenotypic characterization of these populations by surface markers is now better defined [51]. In human peripheral blood mononuclear cells (PBMCs), the equivalent to M-MDSCs can be defined as $CD11b^{+}CD33^{+}CD14^{+}CD15^{-}HLA\text{-}DR^{-/low}$; PMN-MDSCs subpopulation was described as $CD11b^{+}CD33^{+}CD14^{-}CD15^{+}HLA\text{-}DR^{-/low}$ [48,51]. Lectin-type oxidized LDL receptor-1 (LOX-1) has been proposed as a new marker to distinguish human PMN-MDSCs from circulating non-suppressive neutrophils [52,53]. Recently, a more immature subpopulation was identified - early-stage MDSC (eMDSC) - and defined as $CD11b^{+}CD33^{+}CD14^{-}CD15^{-}HLA\text{-}DR\text{-}/^{low}$ Lin^{-} [46,51].

1.3.2. MDSCs-mediated Immunosuppression

The term MDSC presumes suppressive activity which means that immunossupression is a main feature of these cells [46,51]. MDSCs are recognized to interact with a myriad of immune cells as NK and B cells; yet the inhibition of T-cell function is the definition of their suppressive activity [51]. In fact, tumour cells alter immature myeloid cells and exploit their suppressive functions to escape immunosurveillance [46,47].

The main mechanisms implicated in MDSC-mediated immunossupression can be included in major groups and seem to be preferentiably used by different subpopulations [46,47,48].

1) *Lymphocytic nutrient depletion*: L-arginine is an aminoacid crucial for the production of the CD3ζ-chain, an important component of the T-Cell Receptor (TCR). The deplection of L-arginine via the enzyme arginase 1 (ARG-1) results in down-regulation of the CD3ζ-chain in the TCR complex and proliferative arrest of antigen-activated T-cells. The expression of ARG-1 is under the control of prostaglandin E_2 (PGE_2) and Th2 cytokines (IL-4, IL-10, IL-13) [46,47,48];

2) Creation of Oxidative Stress: Reactive oxygen species (ROS) and reactive nitrogen species (RNS), as peroxynitrite (PNT) and hydrogen peroxide, are mainly produced by PMN-MDSCs [46,48,50]. The sources of ROS and RNS in these cells are mitochondria, NADPH oxidase, the peroxisome, the activity of ARG-1 and inducible nitric oxide synthase (iNOS). PMN-MDSCs promote their suppressive activity in a antigen-specific manner, by desensitizing the TCR and its responsiveness to antigen presenting MHC complexes, and down-regulating the expression of the CD3ζ-chain. M-MDSCs also contribute to oxidative stress by mainly expressing iNOS, the enzyme responsible for nitric oxyde (NO) production, further contributing to TCR nitration and desensitization [46,47,48,50];

3) Impairment of lymphocyte trafficking: The membrane expression of the protein ADAM17 by MDSCs (belonging to the family of desintegrins and metalloproteinases) was shown to cleave L-selectin on naïve T-cells, impairing T-cell homing and activation in the lymph nodes [46,48]. Also, downregulation and modification of adhesion molecules, as CD44, P-selectin or CCL2, impairs T-cell extravasation and tumor infiltration [48];

4) *Induction of other immunossupressive cell populations:* MDSCs are able to induce the expansion of immunossupressive Tregs *de novo* or by promoting differentiation from

naïve $CD4^+$ T-cells and transdifferentiation from Th17 lymphocytes. In cancer, Tregs promote tumorigenesis by suppressing T-cells, and Th17 lymphocytes promote cell survival and angiogenesis [50]. The mechanisms involved on these phenomena are not completely clear but may involve cell-cell interaction and prodution of cytokines such as interferon (IFN)-γ, transforming growth factor (TGF)-β and interleukin (IL)-10. MDSCs were also shown to promote a shift from M1 to suppressive M2 phenotype in macrophages [52];

5) *Expression of immune checkpoint regulators:* Recent data has shown that MDSCs express checkpoint molecules such as programmed death ligand-1 (PDL-1), which interact with PD-1^+ T-cells, inducing a state of anergy and apoptosis [50,52].

In 2016, recommendations for the standardization of MDSCs nomenclature and characteristics were published by Bronte *et al* [51]. These authors proposed an algoritm to identify MDSCs in which, additionally to the phenotypic criteria described before, MDSCs must, at least, demonstrate the ability to inhibit T-cell activity, measured by either T-cell proliferation and/or inhibition of IFN-γ production [51].

1.3.3. MDSCs Accumulation and Activation

Pluripotent hematopoietic stem cells (HSCs) are tightly regulated by intrinsic and environmental factors. These cells have the ability to self-renew and differentiate; however this delicate balance can be disturbed under pathological conditions, such as chronic inflammation and cancer, leading to MDSCs expansion [49]. MDSCs generation involves two different phases: accumulation and activation [44,54]. Accumulation of MDSCs is achieved by blockade of terminal differentiation of immature myeloid cells, which is controlled by soluble

factors like granulocyte-macrophage (GM)-CSF, granulocyte-colony stimulating factor (G-CSF), macrophage (M)-CSF and vascular endothelial growth factor (VEGF) [29,52,55]. The release of G-CSF and GM-CSF will trigger the activation of the Janus kinase (JAK)/ signal transducer and activator transcription (STAT) downtream pathway. STAT3 is a transcription factor that is translocated to the nucleus after phosphorylation by JAK kinases, upregulating anti-apoptotic factors such as B-cell lymphoma XL (BCL-XL), MYC, cyclin D1 and survivin [47,54]. Furthermore, this pathway is also involved in the regulation of the CCAAT/enhancer-binding protein-B (C/ERPB) transcription factor, which influences normal myelopoiesis and plays a role in controlling differentiation of myeloid progenitors [47,54].

Inflammation-associated VEGF, secreted by cancer cells in the tumour microenvironment (TME), attracts MDSCs from the blood marrow to the bloodstream, contributing also to MDSCs expansion [48,49]. VEGF production interferes with the differentiation and maturation of granulocyte-macrophage precursors and, together with TGF-β, leads to the development of suppressive myeloid cells and the induction of immunossupressive tumor-associated macrophages (TAM) [56].

MDSCs activation is mediated by the sustained secretion of cytokines in the TME such as IL-1β, IL-6, IL-10, IFN-γ, TGF-β and damage-associated molecular patterns (DAMPs), which are endogenous ligands released in response to hypoxia, cellular stress and tissue injury [53,55]. *In vitro*, the induction of $CD33^+$ MDSC-like cells from healthy peripheral mononuclear blood cells was achieved in the presence of GM-CSF alone or in combination with IL-1β, IL-6, TNF-α or VEGF [54,57].

Tumour cells are known to produce a variety of inflammatory mediators and, other cells in the TME, such as fibroblasts and stromal immune cells, also produce these factors [56]. Interleukin-1β plays a major role in the activation of MDSCs. This was demonstrated by

inoculation of IL-1β secreting tumour cells in mice, which in contrast to the inoculated non-IL-1β producing tumour cells, induced the production of significantly higher levels of Gr^+CD11b^+ MDSCs [58]. Furthermore, IL-1β was shown to upregulate the production of TNF-α, which increases the suppressive abilities of MDSCs, and stimulates the production of several other cytokines as IL-5, IL-10 and IL-13 [56,58]. Another key factor in this process is IL-6 and increased levels of this cytokine correlate with MDSCs frequency and suppressive activity [56]. MDSCs express IL-6 receptor (IL-6R), which activates the STAT3 pathway, contributing to the suppressive potential of MDSCs and promoting their proliferation [50,56,58]. Previous reports showed that blockage of IL-6 or IL-6R, in mouse tumour models, resulted in significant reduction of tumour infiltrative MDSCs and tumour development [56].

Several pathways downstream to STAT3 seem to be involved in the expansion of MDSCs. Activation of STAT3 in hematopoietic progenitor cells upregulates the proinflammatory proteins S100A8 and S100A9, which are calcium-binding proteins released by neutrophils and monocytes, in order to amplify the inflammatory cascade and serve as chemoattractants for leucocytes [48,54,58]. S100A8/A9 proteins also contribute to the blockage in myeloid precursor differentiation and play an important part in the chemoattraction of MDSCs to tumor sites, through the activation of the nuclear factor kappa-light-chain-enhancer of activated B-cells (NF- κB) pathway [52,54,56,58].

1.3.4. MDSC role in tumour progression and metastasis

Tumour-derived factors contribute to the expansion and activation of MDSCs, which in turn, support tumour development, resulting in a complex crosstalk [49]. In addition to immunossupressive functions, MDSCs play a direct role in tumour progression, neoangiogenesis and metastasis [46,49,56].

In a highly hypoxic TME, hypoxia inducible factor (HIF)-1α signaling cascades lead to VEGF expression, an important family of signaling proteins involved in both vasculogenesis (de novo formation of vessels by recruitment of bone marrow derived endothelial progenitor cells) and angiogenesis (formation of vessels from pre-existing endothelial cells) [48,49,56]. MDSCs themselves secrete VEGF, creating a positive feedback loop, able to sustain their expansion and their proangiogenic activity [48]. Furthermore, MDSCs were reported to promote tumoral progression and metastasis by secreting multiple matrix metalloproteinases (MMPs), especially MMP9 [46,55,56]. These proteolytic enzymes promote extracellular matrix degradation with consequent invasion of the stroma and intravasation of tumour cells into the bloodstream [49].

MDSCs were also demonstrated to play an important role in the formation of the pre-metastatic niche, defined as the celular and soluble microenvironment settled in a secondary organ to prepare the arrival of circulating tumour cells [55,56,59]. The pre-metastatic niche has become the new paradigm for initiation of the metastatic process and involves a complex interaction between cells of different lineages, blood flow, soluble factors, extracellular vesicles and extracellular matrix [59]. Tumour niches produce a myriad of different chemokines (small signaling molecules that regulate attraction and trafficking of various cells), implicated in the recruitment of MDSCs [48,56,59]. The spectrum of chemokines produced is dependent on the tumour and affects different MDSCs subsets [56]. C-C motif chemokine ligand 2 (CCL2) is a well-characterized chemokine responsible for the mobilization and migration of M-MDSCs through chemokine receptor 2 (CCR2) in several mouse tumour models [48,56,59]. Similarly, chemokine IL-8 or CXCL8 (C-X-C motif ligand 8) is an attractant produced by tumour cells, leading the accumulation of MDSCs via G protein-coupled C-X-C motif chemokine receptors 1 and 2 (CXCR1, CXCR2), in the gastric and ovarian TME [56]. Other

investigations reported the roles of CCL3, CCL5, CCL9 and CCL12 in attracting and maintaining MDSCs in the tumoral niche, in a variety of tumour animal models [48,56,59]. In particular, CCL5 was shown to activate the HIF-1α signaling pathway, leading to upregulation of VEGF and consequent MDSCs expansion [56].

Tumour regulation of MDSCs is bidirectional and results in a crosstalk that promotes tumour progression and metastasis. The expansion of MDSC populations and correlation with clinical outcomes has been reported in both solid and hematologic malignancies, implying the concept that these cell populations are important contributors to cancer immunotolerance and failure of anti-tumour activity [51]. Growing evidence suggests the association between MDSCs burden and poorer outcomes in cancer patients [61,62]. A recent meta-analysis, that included 1864 patients with a variety of cancers, showed that an elevated frequency of MDSCs was associated with shorter overall survival and progression-free survival rates [62]. Furthermore, MDSCs have been implicated in resistance to anti-cancer treatments and the efficacy of ICIs negatively correlated with the levels of MDSCs. In metastatic cutaneous melanoma, circulating MDSCs levels predicted clinical response to ipilimumab (monoclonal antibody against CTLA-4) and higher level of M-MDSCs prevented ipilimumab-stimulated activation of T-cells, resulting in poorer clinical responses [55].

1.3.5. MDSCs and Uveal Melanoma

The induction of MDSCs in UM, has been a proposed mechanism for immune evasion, poor prognosis and treatment resistance [26]; however, only a few studies regarding the role of MDSCs in UM have been published. One *in vivo* study with UM patients showed an expansion in the number of $CD11b^+$ myeloid cells in the bloodstream of uveal melanoma patients, compared to healthy controls; those cells were mainly $CD11b^+CD15^+CD68^-$ and

$CD11b^+CD15^-CD68^-$ [62]. The authors also showed a significant reduction in the CD3ζ chain expression on circulating T-cells, an important component of the TCR, traducing impairment of T-cell function. Furthermore, the reduction in CD3ζ chain expression significantly correlated with the increased levels of $CD11b^+$ cells, which could indicate the ability of MDSCs to suppress anti-tumoral T-cell function [62]. The authors also characterized infiltrating leukocytes in primary UM tumors and showed that both $CD8^+$ and $CD11b^+$ cells were present within the TME of enucleated UM samples. $CD11b^+$ cells expressed majoritarily CD68 (macrophagic marker) but not CD15, which contrasted with the $CD11b^+$ expanded populations in the bloodstream of these patients [62]. Also, infiltrating $CD8^+$ lymphocytes showed reduced expression of the CD3ζ chain, equivalent to what was observed in the circulation. Based on these data, the authors suggested that myeloid cells infiltrating the tumor were mainly suppressive TAMs that inhibited CTL responses [62].

Regarding metastatic UM, Achberger S *et al* showed the presence of an increased number of PMN-MDSCs populations in patients developing UM metastasis. In the bloodstream of six UM patients, these authors demonstrated a statistically significant increase of circulating $CD11b^+CD15^+CD14^-$ cells after the development of metastasis, compared to their respective levels at diagnosis [63].

Taken together, the aforementioned data suggests that MDSCs may contribute to UM progression and possible failure of novel immunotherapy strategies, making these cells interesting anti-cancer targets.

1.4. Cyclooxygenase-2 (COX-2)

COX-1 is constitutively expressed in human cells and COX-2 is an inducible enzyme, associated with inflammation and carcinogenesis [64]. COX-2 pathway is preferentially

associated with the synthesis of PGE_2 and PGI_2 and PGE_2 is the main mediator of COX-2 role in cancer [64,65]. Several human tumours have shown COX-2 overexpression including colorectal, breast, stomach, lung and pancreas. The reported roles of COX-2 and PGE_2 in tumor development and progression include: cell growth, apoptosis resistance and cell survival, angiogenesis stimulation through upregulation of VEGF, promotion of an inflammatory microenvironment, extracellular matrix invasion via upregulation of MMPs and maintenance of cancer stem cell activity [64,65,66]. COX-2 also plays a role in immune dysfunction, promotes type-2 immunity responses (classically associated with production of IL-4, IL-5, IL-9 and IL-13 and observed in tissues during allergic inflammation and helminthic infections), and is responsible for the suppression of dendritic cells (DC), natural killer (NK) cells and type-1 immunity (classically identified with cell-mediated cytotoxicity). A recent study showed that supernatants from cutaneous melanoma cell were capable of subverting the pattern of inflammatory cytokines derived from mouse bone-marrow derived mononuclear cells and those effects were dependent on PGE_2 and COX enzymes [66]. The same authors, using an immunocompetent mouse model of cutaneous melanoma, showed that tumor derived PGE_2 impaired the accumulation of $CD103^+$ DCs and suppressed their activity and cytokine production. Furthermore, genetic ablation of COX rendered tumor cells unable to produce PGE_2 and allowed T-cell control of tumor growth [66].

Based on the aforementioned, inhibition of COX-2 emerged as an ideal target for cancer treatment and the first clinical trials evaluating the role of selective anti-COX-2 medications occurred in the 1990s. Thereafter, Celecoxib was shown to reduce the risk of colon adenomas in patients with familial adenomatous polyposis but increased the risk of cardiovascular events [67]. Nevertheless, interest in anti-COX-2 antitumor effects has been growing, mainly

after observation that their administration with thromboxane A_2 (TXA_2) synthase inhibitors could alleviate the cardiovascular side effects observed [67].

1.4.1. COX-2 and Uveal Melanoma

COX-2 has been identified in a great number of human malignancies. An immunohistochemical study of 40 human UM samples, COX-2 expression was shown in 58% of cases and was associated with histopathological features of poor prognosis such as epithelioid cell type, closed vascular loops and TILs [68]. The majority of COX-2 expression was located around blood vessels, a finding that is consistent with the role of COX-2 in angiogenesis [68]. Cryan *et al* related the expression of COX-2 with reduced survival rates, showing a positive association between metastatic death and both intensity and extent of COX-2 staining [69]. The authors also showed association between high intensity of COX-2 staining and the presence of epithelioid cells [69]. An *in vitro* study with UM cell lines showed higher proliferation rates when transfected to express COX-2, compared to their non-transfected counterparts with the exception of one cell line, which confirms the pro-proliferative role of COX-2 in tumor cells [70].

Regarding the interaction between immune and tumor cells, an immunohistochemistry study showed that COX-2 was also expressed in infiltrating TAMs and more abundant in those cells than in UM cells [71]. Consequently, a greater amount of macrophage infiltration was associated with a greater degree of COX-2 immunoexpression. To further study this interaction, Marshall JC *et al* evaluated the nitric oxide (NO) production by macrophages after the addition of melanoma conditioned medium (MCM) [70]. Using five transfected UM cell lines to express COX-2, they added their MCM to a monocyte cell line and observed that four of the cell lines significantly reduced NO production from the monocytes/ macrophages [70].

The decrease in NO production was significantly different when the MCM medium originated from non-transfected cell lines, showing a relevant role of COX-2 on immune dysfunction. Furthermore, the addition of Amfenac (the active metabolite of Nepafenac, a COX-2 inhibitor) to MCM of the four UM cell lines partially rescued the macrophage NO production. Interestingly, the addition of Amfenac decreased the proliferation of UM cell lines transfected to express COX-2, but also those not transfected [70]. The authors hypothesized that some COX-2 inhibitors may act through COX-2 independent mechanisms, which have been widely reported in the literature [64,70].

As for *in vivo* studies, Marshall *et al* used a previously described human UM rabbit model immunosuppressed with cyclosporine. The authors injected in the suprachoroidal space, one million 92.1 UM cells. The obtained *post-mortem* tumor specimens showed diffuse COX-2 immunoexpression, in contrast with the injected cell line, which did not express COX-2 *in vitro*, further indicating that the full TME may be necessary to induce COX-2 expression [72]. This work also revealed that the use of topical Nepafenac in the experimental group delayed progression of intraocular tumors and development of lung metastasis, in comparison to the control group [72]. The most remarkable finding was the significantly lower cumulative incidence of micrometastasis in the treated group, suggesting that tumor cells took longer to reach the lungs and establish secondary lesions [72].

1.4.2. COX-2, PGE_2 and MDSCs

COX-2 and PGE_2 are produced by many tumors and greatly contribute to the inflammatory TME [58,73]. As previously discussed, a proinflammatory *millieu* plays an important role in the expansion and activation of MDSCs, but the latter are also producers of infllamatory mediators. Prostaglandins, in particular PGE_2 have been implicated in MDSC-mediated

immunossupression [54]. Specific cell surface G-protein-coupled receptors for PGE_2, designated EP1–4, are present in MDSCs and their activation was shown to induce expression and activity of ARG-1 and NOS, which, as reviewed before, is responsible for the dysfuntion of the TCR and the production of ROS and RNS [64,74]. In a lung cancer mouse model, PGE_2 production from tumor cells induced ARG-1 expression in MDSCs, by signaling through the E-prostanoid (EP)-4 receptor [75]; the genetic and pharmacological inhibition of COX-2 induced an antitumor T-cell response. Another study using an animal model, inoculated four different murine mammary cancer cell lines and showed a direct correlation between COX-2 and ARG-1/ NOS-2 transcript levels in isolated tumor non-parenchymal cells. This same study revealed that the frequency of splenic MDSCs directly correlated with splenic COX-2, NOS-2 and ARG-1 mRNA levels, whereas COX-2 and NOS-2 transcript levels inversely correlated with splenic $CD3^+$ frequencies [76]. The authors thus propose that COX-2 secreted by tumor cells activate MDSCs upregulating NOS-2 and ARG-1 expression which, in turn, impair T-cell function. Lechner M *et al* demonstrated *in vitro,* the inhibition of tumour-induced $CD33^+$ MDSCs by Celecoxib and Celecoxib analogs, via a non-COX-2 dependent mechanism [77]. The authors reported the effects of MDSCs co-cultured with T-cells in the presence and absence of drug, by evaluating T-cell proliferation. The reversal of MDSCs suppressive effects on T-cell proliferation was achieved by COX-2 inhibitors, and persisted after PGE_2 rescue [77]. The treatment of $CD33^+$/T-cells co-cultures with Celecoxib showed a decrease of MDSCs suppressive activity, that correlated with decreased transcript levels of STAT3 and HIF-1α; no effect was observed in $CD11b^+$/ T-cell co-cultures [77].

Additionally to MDSCs-mediated immunossupression, COX-2/PGE_2 also play a role in MDSCs expansion and activation. A EP-2 receptor knockout mouse model of metastatic mammary carcinoma showed delayed tumor growth and lower number of suppressive

$CD11b^+Gr1^+$ MDSCs compared to wild-type mice, suggesting the role of PGE_2 on MDSCs induction, through the EP-2 receptor [73]. Furthermore, the treatment with a COX-2 inhibitor reduced primary tumor growth and MDSC accumulation.

A murine mesothelioma model, treated with dietary Celecoxib, showed a significantly lower number of MDSCs in the spleen, compared with the mice receiving control diet. In addition, not only the number of MDSCs was affected by the treatment, but also the production of ROS by those cells [78]. The authors also demonstrated that anti-tumor CTL responses, induced by dendritic cell immunotherapy, were affected by suppressive MDSCs and, subsequently restored in mice receiving Celecoxib. Based on their findings, Veltman *et al* revealed that dietary administration of Celecoxib prevented local and systemic expansion of MDSCs and reversed T-cell tolerance, in an animal model of mesothelioma [78].

The COX-2/PGE_2 axis was additionally demonstrated to suppress the differentiation of human monocytic precursors into functional Th1-inducing $CD1a^+$ DCs. The addition of synthetic PGE_2, or other COX-2 activators such as IL-1β and IFN-γ, blocked the differentiation of DCs, promoting the development of $CD1a^-$ $CD14^+$ cells. The latter highly expressed PGE_2, indoleamine 2,3-deoxygenase (IDO)-1, NOS-2 and IL-10, suppressive factors tipically produced by MDSCs, establishing a positive feedback loop between PGE_2 and COX-2 [79]. Similarly, studies with primary cells from ovarian cancer patients, in a transwell system or using conditioned medium (CM) from cancer-ascites cells, were capable to block DC differentiation (traduced by the loss of $CD1a^+$ marker) and redirect them into a $CD1a^-CD14^+$ phenotype. Likewise, those $CD1a^-CD14^+$ cells expressed high levels of ARG-1, IDO1, NOS-2, IL-10 and COX-2 mRNA [79].

Collectively, the presented data indicate that COX-2/ PGE2 contribute to immune evasion and resistance to immunotherapy [64]. Tumor production of COX-2 maintains elevated levels

of MDSCs, blocking anti-tumoral immunity and allowing the malignant cells to proliferate (64). This provides a rationale for therapeutic targeting of COX-2 expression to boost immune surveillance and immunotherapy of cancer.

2. PURPOSE

The mechanisms regulating UM immune escape remain obscure and are probably responsible for its progressive course, poor prognosis and treatment resistance. This project aims to contributes to better understand the role of the innate immune system in UM.

2.1. Global Aim:

The main purpose of this project is to study the interactions between MDSCs and UM cells *in vitro*. Our primary aim is to *evaluate the ability of UM cell lines, with typical UM mutations and generated from primary or metastatic disease, to induce the expansion of MDSCs from peripheral blood mononuclear cells* (PBMCs) of healthy volunteers, *and compare them in terms of phenotype and suppressive ability.*

2.2. Specific Aims:

a) To define a methodology to induce $CD11b^{+}CD33^{+}$ myeloid cells from co-cultures of PBMCs and UM cell lines

b) To characterize the phenotype of the induced $CD11b^{+}CD33^{+}$ myeloid cells, and evaluate their ability to suppress autologous T-cell proliferation

c) To evaluate the effect of different concentrations of a selective COX-2 inhibitor (Celecoxib) on the induced $CD11b^{+}CD33^{+}$ cells suppressive activity

d) To characterize the panel of cytokines released in the supernatants of PBMCs/ UM co-cultures

3. MATERIAL AND METHODS

3.1. Cell Lines and Cell Culture

Cell line MEL270, established from a primary human UM, and cell line OMM 2.5 from a UM liver metastasis of the same patient, originally derived by Tim Murray at the Bascom Palmer Eye Institute, were kindly gifted by Dr. Vanessa Morales (University of Tennessee). The 92.1 primary UM cell line was kindly provided by Dr. Antonia Saornil from the Instituto Universitario de Oftalmobiología Aplicada, University of Valladolid. These cell lines have been extensively characterized regarding histopathology, mutations, chromosome status, HLA type, and expression of melanocyte markers, hence its frequent use in UM cell line experiments [80]. MP-41 (ATCC CRL-3297) UM cell line was acquired from American Type Culture Collection (ATCC, Manassas, VA, USA). The SCCL-MT1 cell line was kindly gifted by Dr. Alan L. Epstein (University of Southern California) and was previously described as a head and neck carcinoma cell line with prominent ability to induce potent $CD33^{+}$ suppressive MDSCs [77]. Tumor cell line authenticity was evaluated by cytogenetics and surface marker analysis performed at ATCC or in our laboratory.

All cell lines were cultured in the universal medium [Roswell Park Memorial Institute (RPMI) 1640 medium (Corning Mediatech, Inc. Manassas, VA,USA), supplemented with 10% fetal bovine serum (FBS) (Corning); 2 mM L-Alanyl-LGlutamine (Glutagro, Corning); 1 mM sodium pyruvate (Corning); 100 IU/mL penicillin (Corning); 100 µg/mL streptomycin (Corning); 10Mm Hepes (Corning), and 0.01mg/mL human insulin (Roche, Indianapolis, IN, USA)]. Cells were maintained at 37°C in a humidified 5% CO2-enriched atmosphere (Thermo Forma Series II Water Jacketed CO2 Incubator; Fisher Scientific Limited, Ontario, Canada). Cell quantifications were performed using a TC20 Automated cell counter (Bio-Rad Laboratories Inc).

3.2. Tumor-associated MDSC Generation

3.2.1. MDSC Induction

Blood samples (40-60mL) were drawn by peripheral venous punctures of healthy volunteers, after obtaining written informed consent. Human PBMCs were isolated with Lymphoprep® and SepMate™ isolation tubes (StemCell Technologies), by a density gradient centrifugation protocol, according to the manufacturer's intructions, within 4 hours after venipuncture. PBMCs were washed, cell number was assessed with an automated cell counter and cell viability by the trypan blue dye exclusion method. PBMCs were resuspended in universal medium.

To induce the MDSCs, co-cultures were established between tumour cell lines and PBMCs. A total of $2x10^5$ tumor cells were seeded into an insert the day before PBMCs isolation. Polyethylene terephthalate transparent membrane inserts with 0.4 μm pores were mounted on 6-well plates (Falcon, Corning) and covered with universal medium. Isolated PBMCs ($5x10^6$/well) were added to the bottom of the 6-well plate (outside the insert), to achieve a tumor: PBMC ratio of 1:25, and cultured for 5 days. PBMCs cultured in medium alone were run in parallel as negative controls.

3.2.2. MDSC Isolation

After 5 days, floating and adherent PBMCs were collected. Adherent cells from the bottom of the 6-well plate were removed using a cell detachment solution to minimize surface protein digestion (Detachin, GenLantis, San Diego, CA). Live Myeloid cells with purities over 95% were isolated by Fluorescence-activated cell sorting (FACS). FACS analysis is used to identify, purify, and quantify cell subsets from a mixture of cells using fluorescent-antibodies directed against known surface molecules.

3.2.3. Suppression Assay

The suppressive function of tumor-educated myeloid cells was assessed by their ability to inhibit the proliferation of autologous T-cells, in a suppression assay. FACS isolated $CD11b^+CD33^+$ were co-cultured with $1x10^5$ autologous FACS isolated CFSE-labeled $CD3^+$ T-cells, in the presence of anti-CD3/CD28 stimulation beads (Dynabeads™, Gibco) in a 96-well plate. The number of $CD11b^+CD33^+$ cells plated was variable, in relation to a fixed number of T-cells, to achieve increasing T:myeloid cells ratios (4:1; 8:1 and 16:1). T-cells were obtained from cryopreserved PBMCs, drawn from the same healthy volunteers. PBMCs were isolated as described in 3.2.1 , resuspended in a 10% dymethyl sulfoxide (DMSO) (Tocris, Oakville, Canada)/ 90% FBS mix and transferred into cryovial tubes for cryopreservation. For the suppressive assay, PBMCs were thawed, labelled with carboxyfluorescein diacetate succinimidyl ester (CFSE) (4 μM, ThermoFisher) and fluorescent-antibodies against $CD3^+$ T-cells (UCHT1, BioLegend) , and finally isolated by FACS.

After 72 hours incubation at 37ºC, 5% CO_2 atmosphere, T-cell proliferation was evaluated by flow cytometry, as dilution of CFSE in labelled T-cells. Suppressive function was evaluated as the ability of $CD11b^+CD33^+$ cells to inhibit autologous T-cell proliferation, resulting in a decreased number of daughter cell generations and unmodified labelling of T-cells. Controls included positive T-cell proliferation control (T-cells alone + proliferation stimuli), negative T-cell proliferation control (T-cells alone), an induction negative control (T-cells + proliferation stimuli + $CD11b^+CD33^+$ from PBMCs cultured in medium only) and an induction positive control (T-cells + proliferation stimuli + $CD11b^+CD33^+$ from PBMCs cultured with SCCL-MT1 cells). Samples were run in triplicate.

3.3. Fluorescence-Activated Cell Sorting

3.3.1. Antibodies and Staining Protocol

The phenotype of *in vitro* generated MDSCs was examined for expression of myeloid and antigen presenting surface markers by FACS. For staining, isolated PBMC were transferred into 5mL polystyrene round-bottom tubes (Corning), washed with staining buffer [phosphate buffered saline (PBS) 1x, supplemented with 2% FBS] and incubated with Fc-receptor blocking agent for 15 minutes at 4°C to prevent nonspecific staining.

Afterwards, a mixture with optimal dilution of the antibodies was added and incubated for 15 minutes, protected from light at 4ºC. PBMCs were stained using the following fluorescently-conjugated monoclonal antibodies: anti-CD11b (ICRF44), anti-CD33-PE (WM-53) (eBioscience), anti-HLA-DR (L243) (BioLegend), anti-CD14 (M5E2), anti-CD15 (HI98) (BD Biosciences) and viability dye eFluor^{TM}780 (eBioscience).

Cells were subsequently washed twice with staining buffer and resuspended for analysis. For T-cell isolation, thawed CFSE-labelled PBMCs were further stained with anti-CD3 fluorescently-conjugated monoclonal antibody (UCHT1, BioLegend) using the described procedure.

3.3.2. Data Acquisition and Analysis

Flow cytometry and live cell sorting was performed at the Immunophenotyping Platform of the Research Institute of the McGill University Health Centre (MUHC-RI). Live cell sorting was performed on the multicolour flow cytometer BD FACSAria^{TM} Fusion, under aseptic conditions. Following initial forward scatter (FS)/ side scatter (SC) discrimination, the gate was set on viable cells. Next, we gated on subpopulations $CD11b^{+}CD33^{+}$, which were sorted and collected in polystyrene round-bottom tubes to be posteriorly plated. To study the phenotype

of $CD11b^{+}CD33^{+}$ cells, gates were further set on HLA-DR^{low} cells, and then on $CD14^{+}$ and $CD15^{+}$ subpopulations.

Prior to acquisition, each antibody was titrated to determine its optimal dilution and fluorescence minus one (FMO) controls were done for all fluorophores. Polystyrene anti-mouse immunoglobulin-coated microparticles were used to optimize fluorescence compensation settings. Unstained cells were used as negative controls. Results were expressed as percentage of positive cells and mean fluorescence intensity.

For T-cell proliferation analysis, cells were collected after 72 hours, stained for viability and with anti-CD3 antibodies, and finally fixed with 2% paraformaldehyde in PBS. After acquisition, CFSE dilution was evaluated by on a flow cytometry histogram (BD FACSCanto II, BD Biosciences) and detected in the blue 488 nm wavelength, 585/42 nm filter. At least $1x10^{5}$ events were acquired and data analyzed with FlowJo™ Software (Tree Star, Ashland, USA). Results were expressed as percentage of T-cell proliferation.

3.4. Cytokines measurements

Supernatants were collected from the induction co-cultures, passed through a 0.2 μm filter and stored in aliquots at -20ºC. In this study, we used Luminex xMAP technology for multiplexed quantification of 14 human cytokines, chemokines, and growth factors.

The multiplexing analysis was performed using the Luminex™ 200 system (Luminex, Austin, TX, USA) by Eve Technologies Corporation (Calgary, Alberta). Fourteen markers were simultaneously measured in the samples using Eve Technologies' Human High Sensitivity 14-Plex Discovery Assay® (MilliporeSigma, Burlington, Massachusetts, USA) according to the manufacturer's protocol. The 14-plex consisted of GM-CSF, IFNy, IL-1β, IL-2, IL-4, IL-5, IL-6, IL-8, IL-10, IL-12p70, IL-13, IL-17A, IL-23, TNF-α. Assay sensitivities of these markers ranged from

0.11 – 3.25 pg/mL for the 14-plex. Quantitation was performed using a standard curve and individual analyte sensitivity values are available in the MilliporeSigma MILLIPLEX® MAP protocol.

3.5. Celecoxib Treatments

Celecoxib (CXB) (Cat 10008672, Cayman Chemical), a selective COX-2 inhibitor, was dissolved in DMSO in a a stock solution of 43mM, aliquoted and cryopreserved at -80ºC. The solution was diluted freshly, prior to each experiment, in universal medium to achieve the concentrations tested in each assay (20 μM, 10 μM, 5μM and 2.5 μM). Celecoxib solution was added to the suppression assay wells, in addition to the isolated $CD11b^{+}CD33^{+}$, autologous CFSE-labelled T-cells and anti-CD3/CD28 stimulation beads.

After incubation for 72h, T-cell proliferation was measured as CFSE-dilution using flow cytometry, as described. In addition to the other controls, positive T-cell proliferation controls with celecoxib were included. Samples were run in triplicate.

3.6. Statistical Analysis

Changes in mean T-cell proliferation in the presence or absence of tumor-educated MDSCs were tested for statistical significance by one-way ANOVAs, followed by Tukey's multiple comparisons test. Mean cytokine levels in cell lines alone and after co-cultures were compared by ANOVAs, with multiple comparison post-hoc testing. Changes in mean T-cell proliferation in suppression assays in the absence or presence of different Celecoxib concentrations were evaluated by ANOVA, followed by Tukey's multiple comparisons test.

An exploratory analysis of the effect of phenotype and cytokine concentrations on T-cell proliferation was evaluated though univariate linear regression models. β-coefficients and 95% confidence intervals (CI) are reported.

Statistical analysis was performed using STATA™ software (version 13.0) and a statistical level of significance $p \leq 0.05$ was considered. Graphs were produced using GraphPad Prism software, version 6 (La Jolla, CA).

4. RESULTS

4.1. Setup of tumor cells/ PBMCs co-cultures

UM cell lines used were similar in terms of growth speed, medium consumption (as determined by color of phenol-containing medium) and time needed for the cells to adhere in tissue culture plates. In contrast, SCCL-MT1 cells growth speed and medium consumption was lower than UM cells. Therefore, to obtain comparable growth conditions, we seeded the cells at different moments in advance, to achieve around 90% of confluence before starting co-cultures. For the setup of co-culture settings, we used two tumor cell lines: SCCL-MT1 and OMM 2.5.

4.1.1. Ratio and Viability of PBMCs and tumor cells in co-cultures

To simulate the co-existence of CTCs and PBMCs in circulation, we assessed the ability of cells to persist in co-culture for different periods of time (5 and 7 days), with a ratio of 1:100. Before starting co-cultures, tumor cells were seeded one day in advance in 1mL of universal medium on a 6-well plate, to allow them to adhere to the plastic. On the day of co-culture start, medium was discarded and replaced with fresh one, and PBMCs were seeded adding another 1mL of fresh universal medium. Culture medium was replaced every 48 hours and, to support culture viability, 20ng/mL of recombinant human (rh) GM-CSF was added at the same time. Presence of rhGM-CSF did not influence the viability and morphology of tumor cells (UM and SCCL-MT1 cells) in isolated cultures, as assessed by trypan blue dye exclusion test (data not shown). PBMCs alone, with addition of rhGM-CSF, were cultured in parallel as induction negative controls. Cells were collected at different timepoints (5 and 7 days). In this experiment, PBMCs obtained from peripheral blood of two different healthy donors were used simultaneously.

PBMCs cultured in the absence of tumor cells showed high percentages of cell viability for both donors at 5 and 7 days. In contrast, daily microscopic examinations of co-cultures of PBMCs with tumor cells showed early deterioration of both, with cell detachment from the bottom of the wells. This was apparent on flow cytometry by cell viability analysis, showing low percentages of live cells (figure 1).

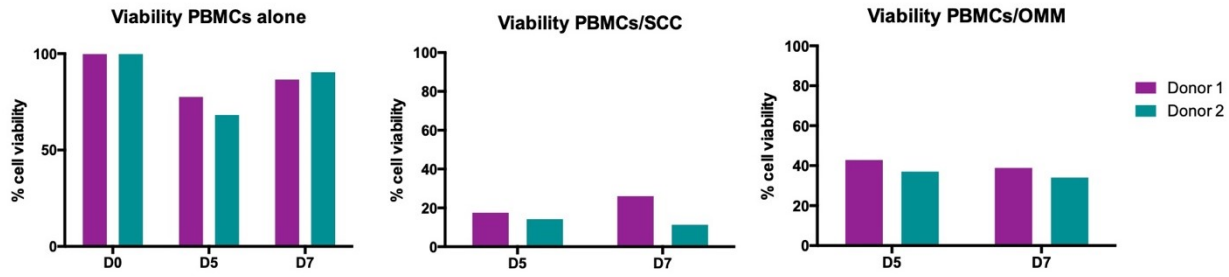

Figure 1: Percentage of live cells for PBMCs cultured in the absence of tumor cells and cultured with SCCL-MT1 and OMM2.5 cells, obtained from 2 different blood donors. Percentage cell viability evaluated at 5 and 7 days is presented.

A different seeding ratio of tumor cells and PBMCs was tested to evaluate cell viability and the ability to induce $CD11b^{+}CD33^{+}$ cells, after 5 days. For this experiment, SCCL-MT1 cell line was cultured in 1:10 and 1:100 ratios with PBMCs. We observed that viabilities in attached and non-attached fractions were similar in both cases but slighly higher in the adherent fraction, for the 1:10 ratio (figure 2). As for the percentage of $CD11b^{+}CD33^{+}$ cells obtained, they were low and similar for both ratios (figure 2).

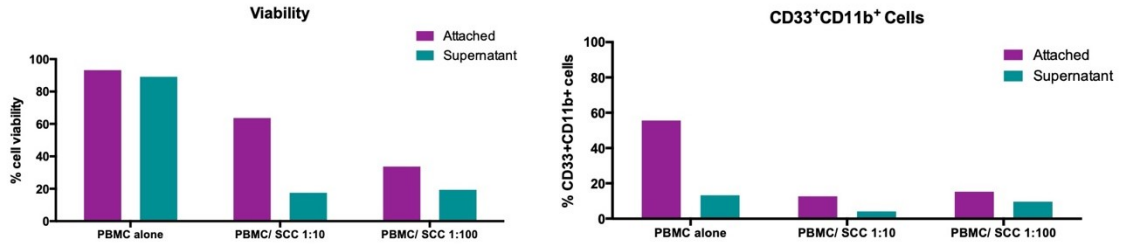

Figure 2: *Left:* Percentage of live cells for PBMCs cultured in the absence of tumor cells and PBMCs cultured with SCCL-MT1 cells, at different seeding ratios. *Right:* Bar graph displaying percentage of obtained $CD33^{+}CD11b^{+}$ cells for PBMCs cultured in the absence of tumor cells and PBMCs cultured with SCCL-MT1, at different seeding ratios.

Co-cultures of tumor cells and PBMCs with cell-to-cell contact resulted in extensive cell death, either for tumor cells and PBMCs, which did not occur when those cells were cultured alone. Based on these observations, we decided to test whether the introduction of a 0.4 μm pore transwell insert to prevent cell-to-cell interaction, was able to increase viabilities and allow establishment of successful co-cultures for 5 days. Co-cultures were assembled as described, seeding PBMCs in complete medium at the bottom of the transwells, at a concentration of $5x10^5$ in each well, and SCCL-MT1 cells inside the inserts at a concentration of $5x10^4$ (tumor cells: PBMCs ratio of 1:10). After 5 days, viabilities of both adherent and non-adherent frations of PBMCs were higher and the percentage of obtained $CD11b^+CD33^+$ cells was also considerably higher (figure 3).

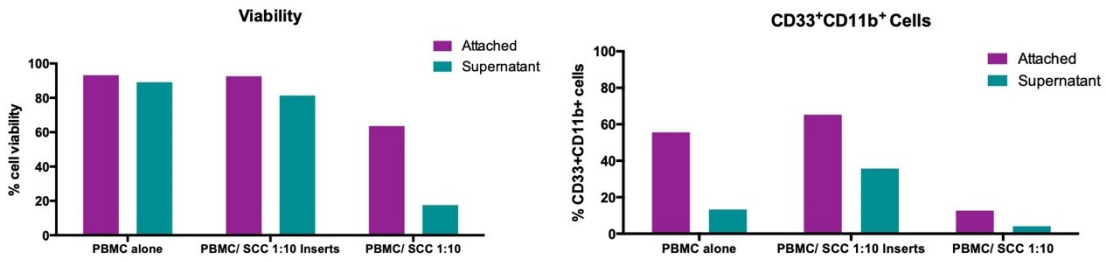

Figure 3: *Left:* Percentage of live cells for PBMCs cultured in the absence of tumor cells and PBMCs cultured with SCCL-MT1 cells, with and without transwell inserts. *Right:* Percentage of obtained $CD33^+CD11b^+$ cells for PBMCs cultured in the absence of tumor cells and PBMCs cultured with SCCL-MT1, with and without transwell inserts.

These results allowed us to define the need for introduction of transwell inserts in co-cultures, to decrease cell death and increase the yield of obtained $CD11b^+CD33^+$ cells.

4.1.2. Introduction of rhGM-CSF in co-cultures

The effect of the introduction of rhGM-CSF in PBMC cultures was also evaluated. Co-cultures in the presence and absence of 20ng/mL rhGM-CSF were seeded, using SCCL-MT1, OMM 2.5 and MEL270 tumor cell lines and PBMCs.

Culturing PBMCs alone with and without supplementation of rhGM-CSF did not influence viability of these cells after 5 days (percent viability for PBMCs alone = 98.4% vs percent viability for PBMCs + rhGM-CSF= 98.7%) (figure 4). The same was observed in co-cultures of PBMCs with different tumor cell lines (figure 4). In what concerns the percentage of isolated $CD33^{+}CD11b^{+}$ cells, we observed that the addition of rhGM-CSF resulted in higher percentages of isolated myeloid cells, when compared to their counterparts cultured without growth factor supplementation (figure 4).

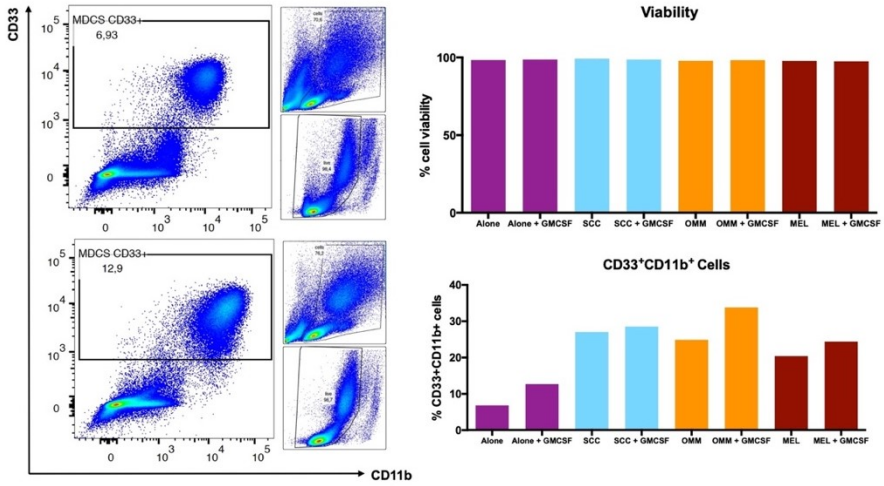

Figure 4: *Left panel:* Flow cytometry gating strategy for $CD33^{+}CD11b^{+}$ myeloid cells obtained from PBMCs cultured in the absence of tumor cells, without rhGM-CSF (superior plot) and with rhGM-CSF supplementation (inferior plot). *Right panel*: Bar graphs displaying percentage of live cells (superior graph) and percentage of obtained $CD33^{+}CD11b^{+}$ myeloid cells (inferior graph) for all the conditions tested

However, culture supplementation with rhGM-CSF influenced the phenotype of the obtained $CD33^{+}CD11b^{+}$ cells, especially for PBMCs cultured in the absence of tumor cells. When analyzing surface markers in PMBCs cultured in medium only, we observed that addition of GM-CSF increased the expression of CD11b in isolated $CD33^{+}CD11b^{+}$ myeloid cells (figure 5). In contrast, when analyzing PMBCs cultured in the presence of SCCL-MT1 cells, the addition of rhGM-CSF did not considerably alter the expression of any of the considered surface markers (figure 5).

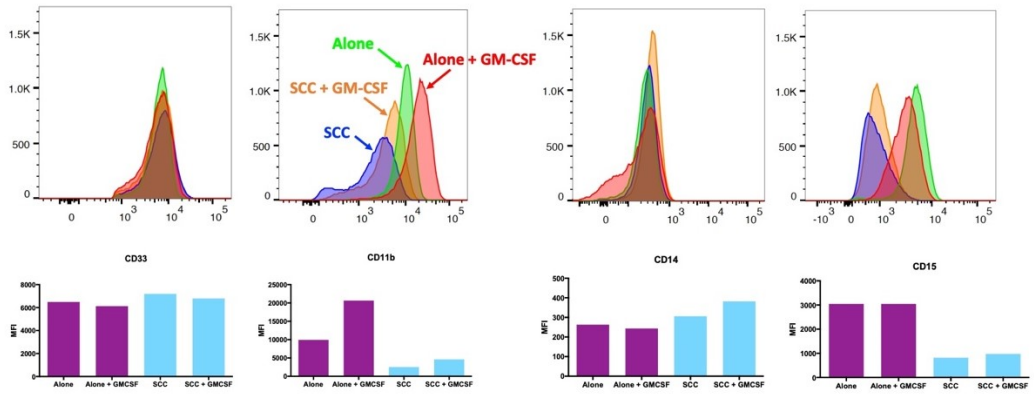

Figure 5: *Superior panel:* Mean fluorescence intensity plotted on histograms for each surface marker (CD33, CD11b, CD14, CD15) on $CD33^{+}CD11b^{+}$ myeloid cells, obtained from different culture conditions. *Inferior panel:* Graphs displaying mean fluorescence intensity for each surface marker (CD33, CD11b, CD14, CD15) on $CD33^{+}CD11b^{+}$ myeloid cells obtained from PBMCs cultured in the absence of tumour cells, with and without rhGM-CSF supplementation and from PBMCs cultured with SCCL-MT1 cells, with and without hrGM-CSF supplementation

Evaluation of the same markers on PBMCs cultured in the presence of different UM cell lines showed similar findings with and without growth factor supplementation (figure 6).

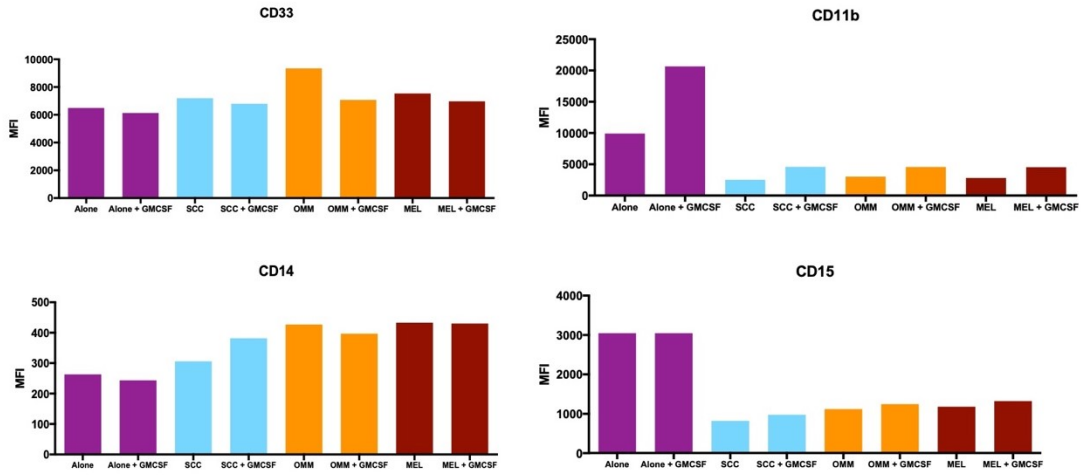

Figure 6: Mean fluorescence intensity for each surface marker (CD33, CD11b, CD14, CD15) on $CD33^{+}CD11b^{+}$ myeloid cells obtained from PBMCs cultured in the absence of tumour cells, with and without rhGM-CSF supplementation and from PBMCs cultured with different tumour cell lines, with and without rhGM-CSF supplementation

These results allowed us to define that rhGM-CSF supplementation was not necessary to increase global viability in cultures for 5 days. Although the addition of rhGM-CSF increased

the percentage of isolated $CD33^+CD11b^+$ myeloid cells from co-cultures, it also introduced artificial changes in surface markers expression.

4.2. Phenotypic characterization of induced $CD11b^+$ $CD33^+$ cells

Co-cultures with PBMCs and tumour cells were assembled as previously described, and PBMCs in medium only alone were cultured in parallel as controls. After 5 days, PBMCs were collected and stained with the previously defined panel of monoclonal antibodies, for FACS live cell sorting. After FS/SC discrimination, the gate was set on live cells and from those, $CD11b^+CD33^+$ cells were gated and examined (gating strategy exemplified in figure 7).

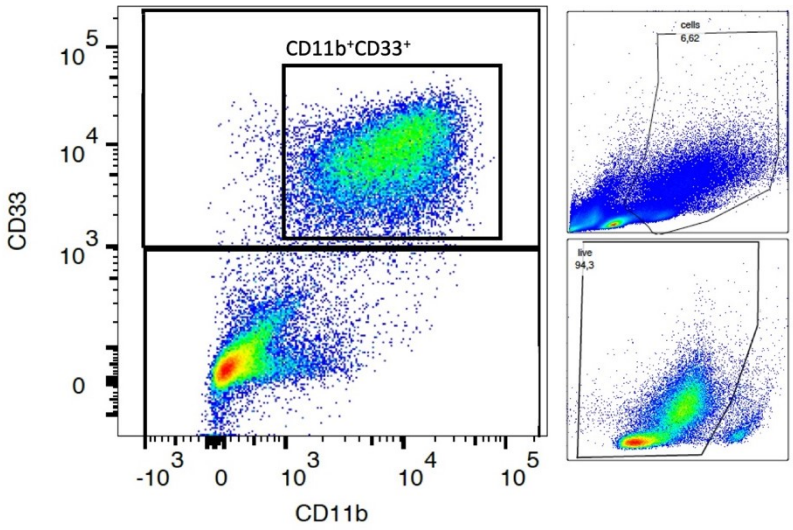

Figure 7: Flow cytometry gating strategy for $CD33^+CD11b^+$ myeloid cells obtained from PBMCs in culture. After FS/SC discrimination, gate was set on live cells and $CD11b^+CD33^+$ cells were isolated

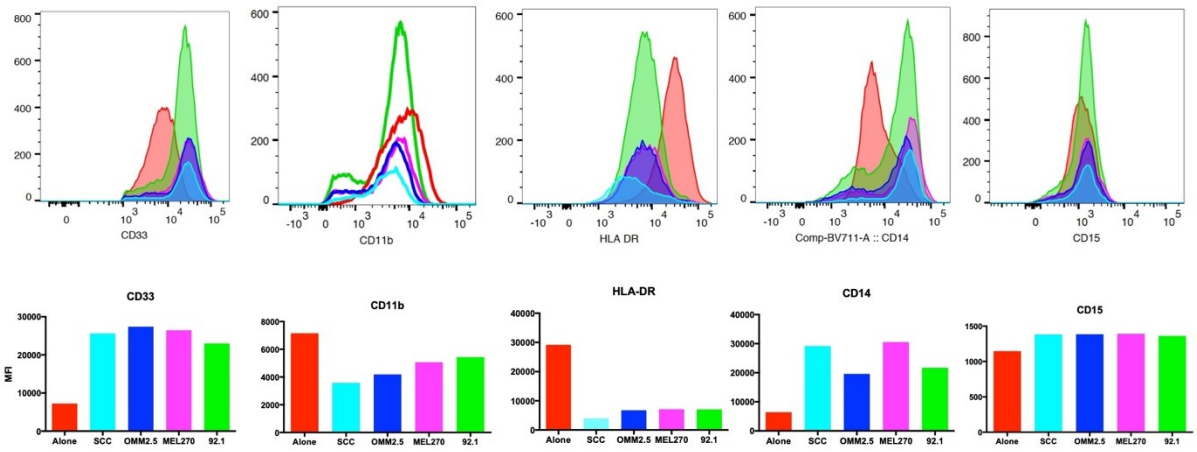

Figure 8: Mean fluorescence intensity for each surface marker (CD33, CD11b, HLA-DR, CD14, CD15) on $CD33^{+}CD11b^{+}$ myeloid cells obtained from PBMCs cultured in the absence and presence of tumour cells, in one representative experiment

Analyzing the expression of surface markers by comparing mean intensity fluorescence (MFI) determined by flow cytometry, allowed us to phenotypically characterize the selected $CD33^{+}CD11b^{+}$ cells (figures 8 and 9). We observed that SCCL-MT1 and UM cell lines OMM2.5, MEL270 and 92.1, share similar surface markers profiles, which contrasts with the phenotype displayed by UM MP41 cells (figure 9).

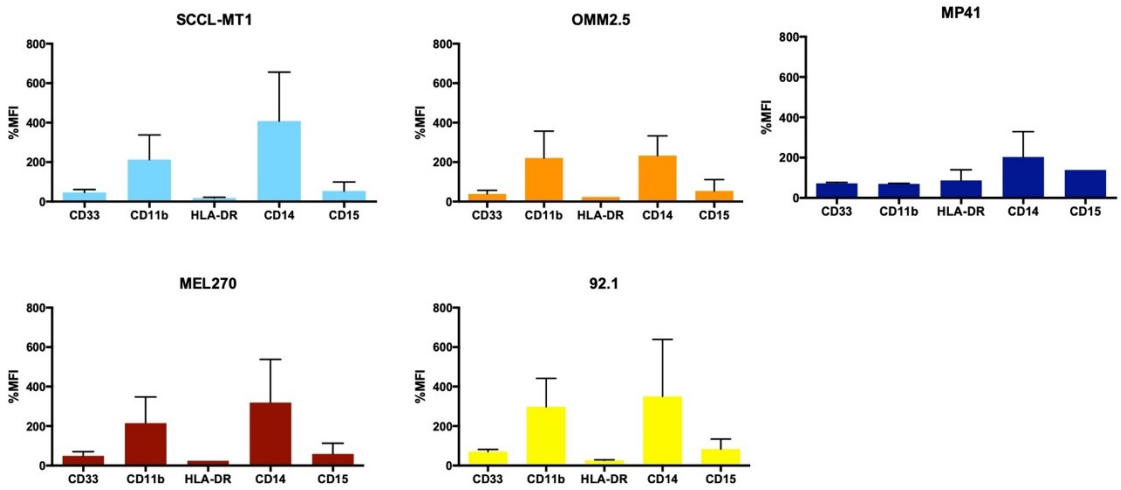

Figure 9: Phenotype of $CD33^{+}CD11b^{+}$ cells induced by tumour cell lines. Data presented as percentage of median fluorescence intensity, in reference to surface markers of $CD33^{+}CD11b^{+}$ cells, obtained from PBMCs cultured in medium only (data from at least 2 different donors; mean $\pm$ SD, except for HLA-DR of OMM2.5 and MEL270, and CD15 from MP41, which correspond to data from only one donor).

For comparison of surface markers MFI among $CD33^{+}CD11b^{+}$ cells, we normalized the data from different experiments and present it in comparison to PBMCs cultured alone.

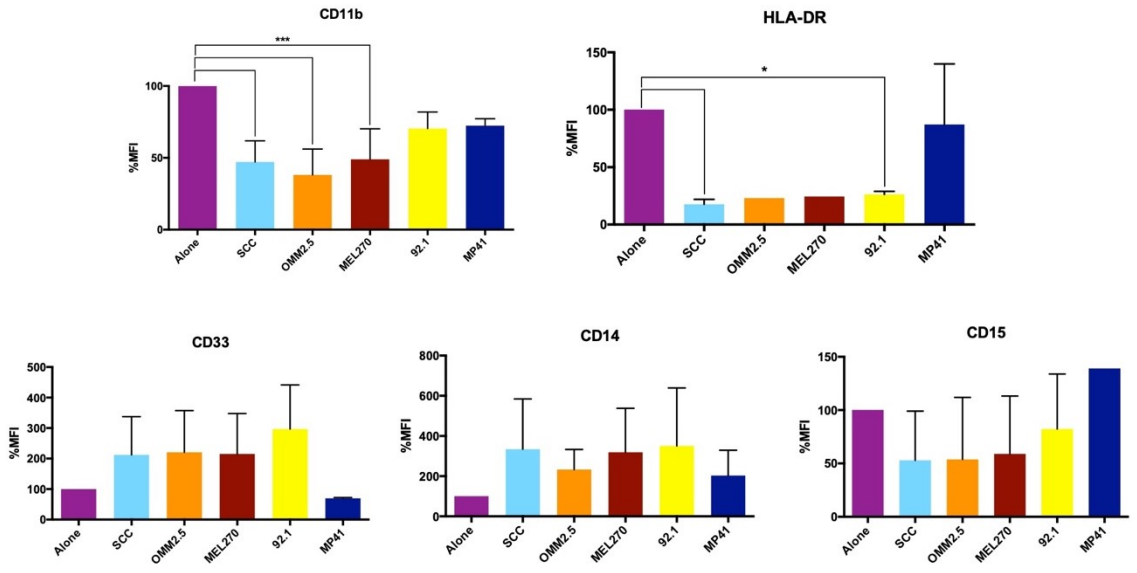

Figure 10: Percentage of median fluorescence intensity per surface marker, in $CD33^{+}CD11b^{+}$ cells induced by different tumor cell lines. Data presented as percentage of median fluorescence intensity, in reference to MFI of PBMCs cultured in medium only (data from at least 2 different donors; mean ± SD, except for HLA-DR of OMM2.5 and MEL270, which corresponds to data from only one donor). Differences in percentage analyzed by ANOVA and Tukey's multiple comparison test. (* and *** indicate statistical significant differences in mean percentage between 2 groups; *p<0.05; ***p<0.001)

For CD11b, we observed that isolated cells from PBMCs cultured with SCCL-MT1, MEL270 and OMM2.5 showed a significant decrease in the percentage MFI of this marker, in comparison to PBMCs cultured in the absence of tumor cells [F(5,15)= 12.08; p= 0.001]. A decrease in the expression of HLA-DR surface marker was also denoted for all the $CD11b^{+}CD33^{+}$ cells obtained from co-cultures with tumor cell lines, except for MP-41 [F(5,7)= 8.14; p= 0.008]. Regarding CD33, there was an increase, not statistically significant, in the percentage MFI of isolated myeloid cells from co-cultures of PBMCs and SCCL-MT1, OMM2.5, MEL270 and 92.1 cells [F(5,15)= 1.88; p= 0.158]. The expression of CD14 and CD15, measured by percentage of MFI, did not show consistent trends among the isolated myeloid cells

[F(5,11)= 0.84; p=0.547] and [F(5,11)= 1.09; p= 0.417], although an increase in the CD14 percentage MFI in comparison to PBMCs cultured alone was observed.

4.6.1 Exploratory analysis of the effect of phenotype on T-cell proliferation

We aimed to explore whether the phenotype of induced $CD11b^{+}CD33^{+}$ cells could predict subsequent T-cell proliferation on suppression assays. For each surface marker (CD11b, CD33, HLA-DR, CD14, CD15), a univariate linear regression model was built. Expression of CD11b, CD33 and HLA-DR were considered predictors of T-cell proliferation (Table 1). For each 1% decrease in CD11b MFI expression, T-cell proliferation decreased by 1.07%; for each 1% increase in CD33 MFI expression, T-cell proliferation decreased by 0.12%; and for each 1% decrease in HLA-DR MFI expression, T-cell proliferation decreased by 0.84%.

Table 1. Univariate Analysis of T-cell proliferation		
Surface Markers	**β-coefficient (95% CI)**	**p-value***
CD11b	1.07 (0.74; 1.41)	**<0.001***
CD33	-0.12 (-0.24; -0.003)	**0.044***
HLA-DR	0.84 (0.55; 1.13)	**<0.001***
CD14	-0.05 (-0.14; 0.05)	0.314
CD15	0.31 (-0.09; 0.70)	0.121

Table 1: Univariate Analysis of T-cell proliferation and myeloid cells phenotype
CI: Confidence interval; *p<0.05

4.3. Setup of the Suppression Assay

To evaluate the effect of myeloid dependent suppression on T-cells, an assay was designed using nonspecific CD3/CD28 stimulation. This assay takes into consideration the ability to induce proliferative arrest of actively dividing T-cell by MDSCs. T-cells were

stimulated using anti-CD3/anti-CD28 superpara-magnetic coated microbeads (Dynabeads™) that allow simultaneous presentation of stimulatory signals to T-cells, allowing their activation and expansion. For the setup of this assay we tested the optimal concentration of Dynabeads™, period of incubation and the need for IL-2 supplementation.

Cryopreserved PBMCs were thawed, labelled with CFSE, incubated for 2.5 and 3.5 days with 1 and 2μL of Dynabeads® per well, in a 96-well plate, in the presence or absence of 30 U/mL rhIL-2. T-cell proliferation was measured as CFSE-dilution using flow cytometry, after gating on $CD3^+$ cells. As illustrated in the following graphs (figure 11), proliferation was dependent on the addition of Dynabeads® and time of incubation, reaching higher values with 2 μL/well, after 3.5 days of incubation. Either 1 and 2μL/ well of Dynabeads® were able to induce proliferation of T-cells and the addition of IL-2 did not show substantial differences (Figure 12). These results allowed us to define the parameters for subsequent suppression assays: T-cells incubation for 3 days using 1 μL Dynabeads® per well.

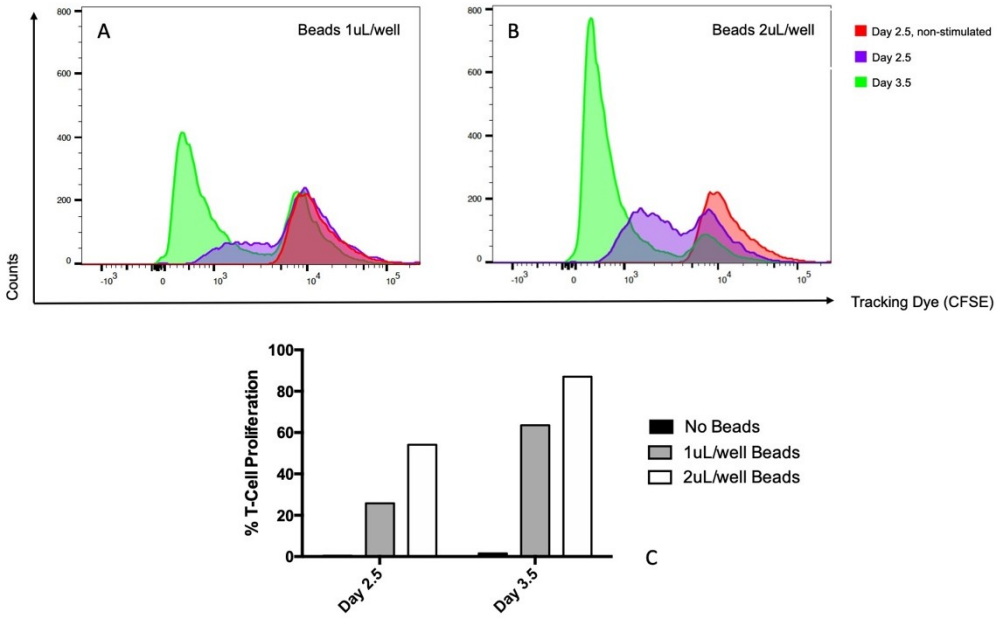

Figure 11: *Superior panel:* Flow cytometry histograms representing $CD3^+$ T-cells proliferation assessed by CFSE dilution. A) CD3+ T-cells unstimulated and stimulated with 1μL of Dynabeads™ for 2.5 and 3.5 days; B) $CD3^+$ T-cells unstimulated and stimulated by 2μL of Dynabeads™ for 2.5 and 3.5 days. C) Graph

comparing percentages of T-cell proliferation on different time-points and with different amounts of anti-CD3/CD28 stimuli.

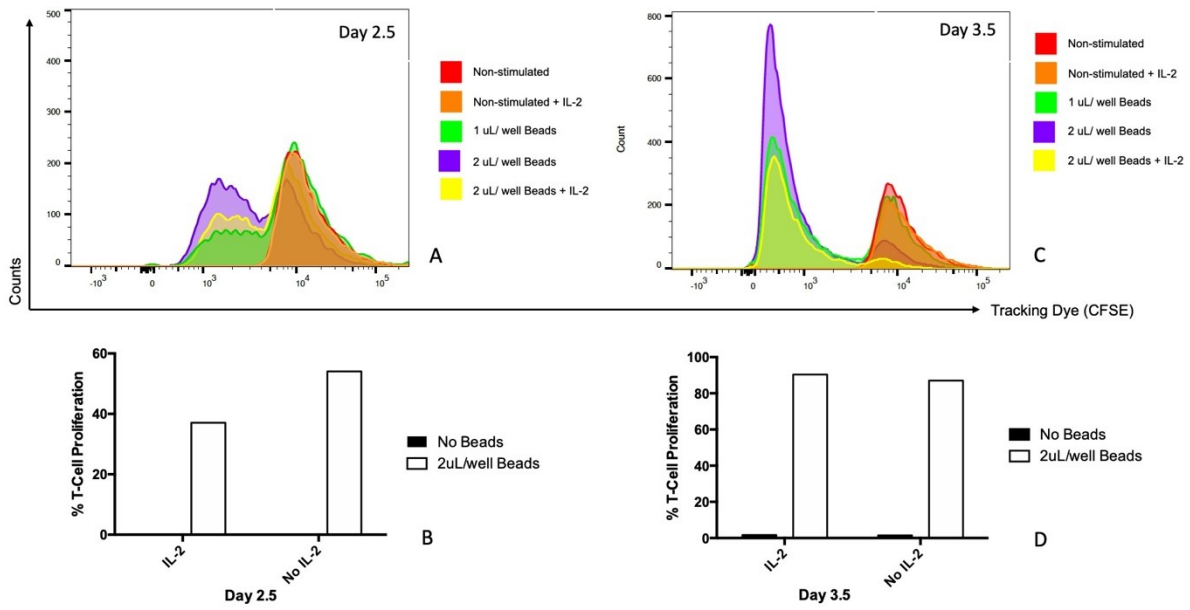

Figure 12: *Superior panel*: Flow cytometry histograms representing $CD3^+$ T-cells proliferation assessed by CFSE dilution. A) $CD3^+$ T-cells unstimulated and stimulated by Dynabeads™ for 2.5 days, with and without the addition of IL-2; B) Graph comparing percentages of T-cell proliferation, with and without IL-2, on the presence or absence of anti-CD3/CD28 stimuli for 2.5 days; C) $CD3^+$ T-cells unstimulated and stimulated by Dynabeads™ for 3.5 days, with and without the addition of IL-2; D) Graph comparing percentages of T-cell proliferation, with and without IL-2, on the presence or absence of anti-CD3/CD28 stimuli for 3.5 days.

4.4. Functional characterization of induced $CD11b^+CD33^+$ cells

Suppressive activity of the induced $CD11b^+CD33^+$ cells was evaluated by the assay previously described. Myeloid cells, at different ratios, were combined with $CD3^+$ T-cells and anti-CD3/anti-CD28 microbeads. Cells were collected after 3 days and analyzed by flow cytometry. After FS/SC discrimination of lymphocytes, the gate was set on live $CD3^+$ cells and from those, proliferation was assessed by CFSE dilution (gating strategy exemplified in figure 13). The obtained data was presented as the percentage of proliferated $CD3^+$ cells and compared by one-way ANOVAs.

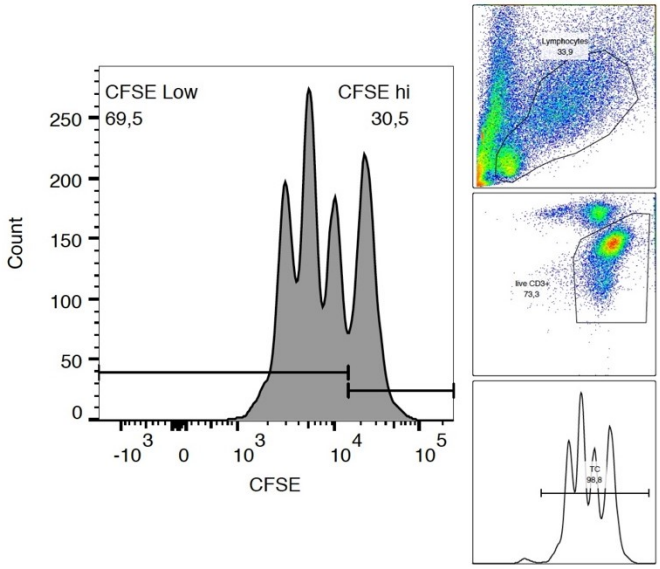

Figure 13: *Left:* Flow cytometry histogram representing $CD3^+$ T-cells proliferation acessed by CFSE dilution. *Right:* Flow cytometry gating strategy for $CD3^+$ cells obtained from suppression assays. After FS/SC discrimination, gate was set on live cells $CD3^+$ cells.

4.4.1. T-cell proliferation with different $CD3^+$/$CD11b^+CD33^+$ culture ratios

T-cell proliferation in the presence of myeloid cells (T-cells + $CD11b^+CD33^+$) was evaluated at 3 different T-cell:$CD11b^+CD33^+$ ratios (1:4, 1:8, 1:16) and compared to proliferation controls (T-cells + anti-CD3/anti-CD28 microbeads). Increasing dilution ratios of T-cells and myeloid cells isolated from PBMCs cultured in the absence of tumor, resulted in increased T-cell proliferation [$F(3,52)= 5.71$; $p= 0.0019$], reaching significance for the highest $CD11b^+CD33^+$ dilution ratio (16:1) ($t=3,55$; $p=0.004$). Conversely, with myeloid cells from PBMCs cultured in the presence of SCCL-MT1 cells, T-cell proliferation was significantly lower for all the culture ratios tested (4:1, 8:1, 16:1) [4:1-t=-5,71; $p<0.001$; 8:1-t=-6.37; $p<0.001$; 16:1-t=-6.22; $p<0.001$] (Figure 14).

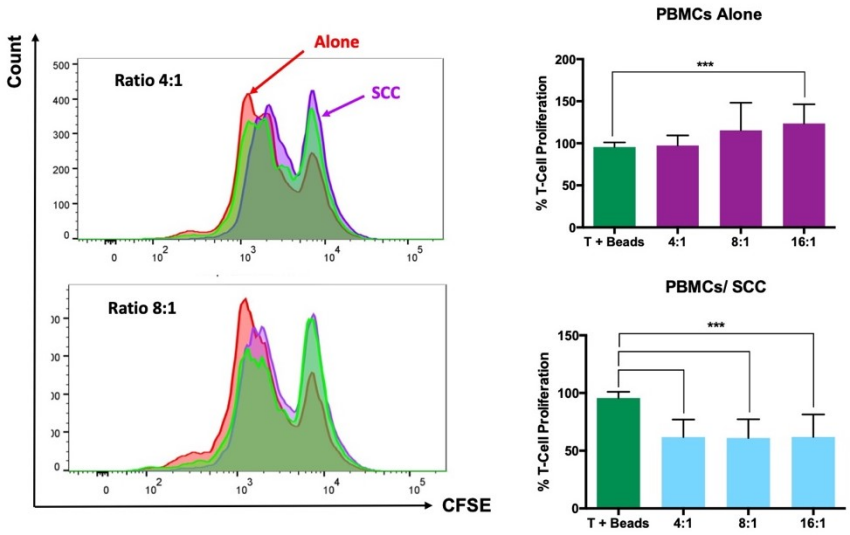

Figure 14: *Left:* Flow cytometry histogram representing $CD3^+$ cells proliferation assessed by CFSE dilution, in suppression assays with myeloid cells from PBMCs cultured alone and PBMCs cultured with SCCL-MT1. Two different culture ratios (T-cells: myeloid cells) are displayed. *Right:* Percentage of T-cell proliferation in suppression assays with myeloid cells from PBMCs cultured alone and PBMCs cultured with SCCL-MT1 cells, in different seeding ratios. Data presented as percentage of T-cell proliferation, in reference to T-cells cultured with proliferation stimuli (data from at least 3 different donors; mean ± SD). Differences in percentage analyzed by ANOVA and Tukey's multiple comparison test. (*** indicates statistical significant differences in mean percentage between 2 groups; ***p<0.001)

Dilution of myeloid cells isolated from PBMCs cultured in the presence of UM cell lines significantly decreased the percentage of T-cell proliferation for the majority of culture ratios and cell lines tested, except for MP41 cell line. After incubation with myeloid cells from PBMCs cultured in the presence of OMM 2.5 cells, T-cell proliferation was significantly lower for all the culture ratios tested (4:1-t=-5,17; p<0.001; 8:1-t=-4.94; p<0.001; 16:1-t=-3.25; p=0.01). The same was observed for MEL270 (4:1-t=-4,36; p<0.001; 8:1-t=-3.22; p=0.011; 16:1-t=-6.22; p=0.04) and 92.1 cell lines (8:1-t=-10.71; p<0.001; 16:1-t=-8.84; p<0.001). Myeloid cells from PBMCs cultured in the presence of MP41 cells did not show significant differences in T-cell proliferation, in comparison to the proliferation control, for the ratios tested [F(2,4)= 1.02; p= 0.42] (Figure 15).

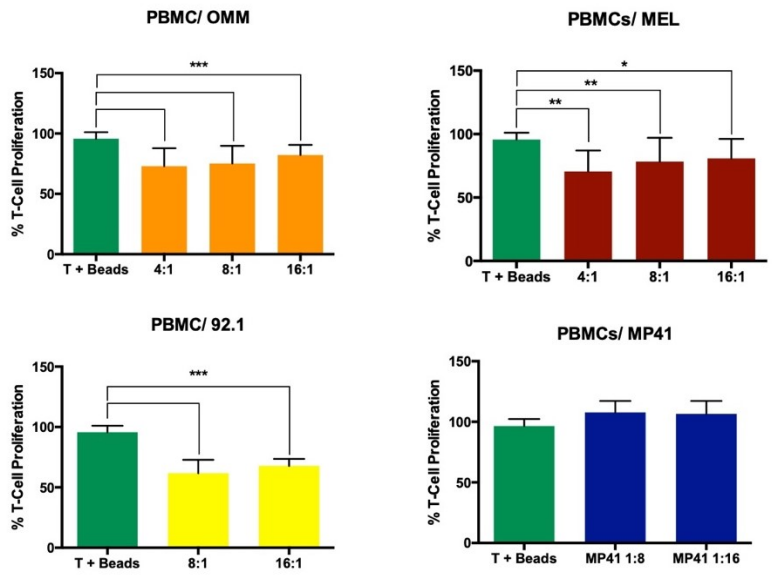

Figure 15: Percentage of T-cell proliferation in suppression assays with myeloid cells from PBMCs cultured with UM cells, in different seeding ratios. Data presented as percentage of T-cell proliferation, in reference to T-cells cultured with proliferation stimuli (data from at least 2 different donors; mean ± SD). Differences in percentage analyzed by ANOVA and Tukey's multiple comparison test. (*, ** and *** indicate statistical significant differences in mean percentage between 2 groups; *p<0.05, ** p<0.01, ***p<0.001)

4.4.2. Comparison between suppressive potencies of induced CD11b⁺CD33⁺ cells

T-cell proliferation in the presence of myeloid cells originated from PBMCs cultured with tumor cell lines showed different suppressive potencies. Considering T-cell proliferation at the 4:1 culture ratio, a statistically significant difference between groups was found [F(4,51)= 14.10; p< 0.001] and Tukey post-hoc test revealed that proliferation was significantly lower in the presence of $CD11b^{+}CD33^{+}$ myeloid cells obtained from co-cultures of PBMCs with SCCL-MT1 (t=-5,24; p<0.001), OMM2.5 (t=-3,59; p=0.006) and MEL270 cells (t=-3,97; p=0.002) (Figure 16). A significant difference between groups was also found for 8:1 [F(6,82)= 15.87; p< 0.001] and 16:1 culture ratios [F(6,82)= 27.49; p< 0.001] (Figure 16). Post-hoc tests showed a significant decrease in T-cell proliferation in the presence of $CD11b^{+}CD33^{+}$ myeloid cells obtained from co-cultures of PBMCs with SCCL-MT1 (8:1-t=-5,20; p<0.001; 16:1-t=-6.32; p<0.001) and 92.1 cells (8:1-t=-4,30; p=0.001; 16:1-t=-4.40; p=0.001). For the 16:1 ratio

culture, a significant increase in T-cell proliferation was noted when they were incubated with myeloid cells obtained from PBMCs cultured alone (t=-5,10; p<0.001) (Figure 16).

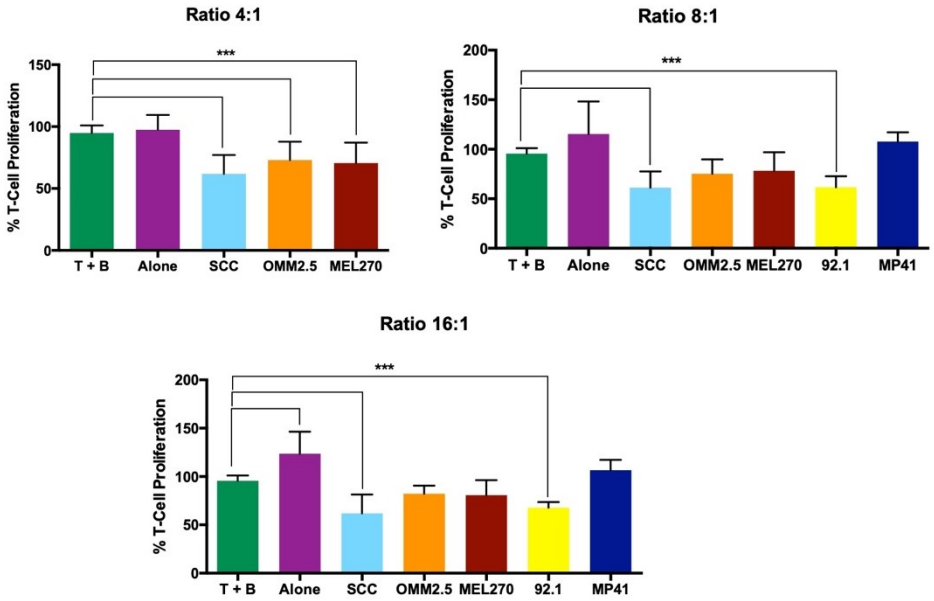

Figure 16: Percentage of T-cell proliferation in suppression assays with myeloid cells from PBMCs cultured alone and PBMCs cultured with tumor cell lines, in different seeding ratios. Data presented as percentage of T-cell proliferation, in reference to T-cells cultured with Dynabeads™ (data from at least 2 different donors; mean ± SD). Differences in percentage analyzed by ANOVA and Tukey's multiple comparison test. (*** indicates statistical significant differences in mean percentage between 2 groups; ***p<0.001)

4.5 Influence of Celecoxib in the suppressive activity of induced CD11b$^+$CD33$^+$ cells

The effect of a COX-2 inhibitor (Celecoxib) in the suppressive activity of the induced CD11b$^+$CD33$^+$ cells was tested by the previously described assay. Myeloid cells were combined with CD3$^+$-cells, anti-CD3/anti-CD28 microbeads and different concentrations of Celecoxib, at different seeding ratios. The obtained data was presented as the percentage of proliferated CD3$^+$ cells.

4.5.1 Setup of Celecoxib concentrations in Suppression Assays

T-cell proliferation was evaluated with addition of decreasing concentrations of Celecoxib (20, 10, 5 and 2.5μM), and compared to the correspondent condition, in the absence of

Celecoxib. For this setup, a 4:1 ratio of T-cells/ $CD11b^{+}CD33^{+}$ myeloid cells in suppression assays was used. For the proliferation control (T-cells + stimulation beads), we observed a statistically significant increase in T-cell proliferation, in the presence of 20μM of Celecoxib (t=3,82; p<0.001), and a significant decrease in T-cell proliferation with Celecoxib 10μM (t=-3,14; p=0.034). In the presence of myeloid cells obtained from PBMCs cultured alone (T-cells + $CD11b^{+}CD33^{+}$), the addition of Celecoxib did not significantly influence T-cell proliferation [F(4,22)= 1.83; p=0.159]. The same observation was made for T-cells cultured with $CD11b^{+}CD33^{+}$ from co-cultures of PBMCs and SCCL-MT1 cells [F(4,22)= 2.39; p= 0.082]. In the presence of myeloid cells obtained from PBMCs cultured with UM cells OMM 2.5, the addition of Celecoxib 5μM significantly increased T-cell proliferation (t=3,21; p=0.029), but no other concentration showed an effect. Based on these results, especially the effects on the proliferation control, we decided to further test the lowest concentration of Celecoxib, 2.5μM.

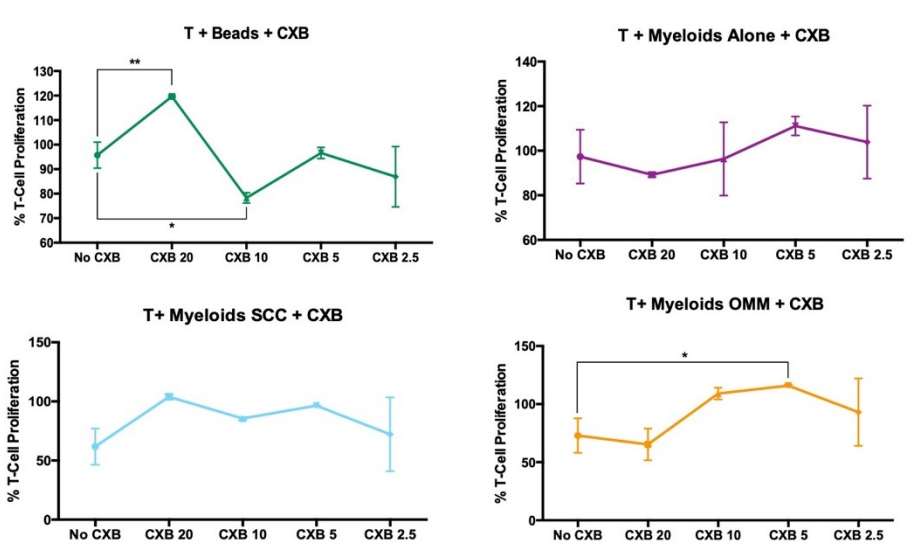

Figure 17: Percentage of T-cell proliferation in different conditions, with addition of serial dilutions of Celecoxib concentration. Data presented as percentage of T-cell proliferation, in reference to T-cells cultured with Dynabeads™ (data from one experiment with triplicates for each condition, mean ± SD). Differences in percentage analyzed by ANOVA and Tukey's multiple comparison test. (* and ** indicate statistical significant differences in mean percentage between 2 groups; *p<0.05, **p<0.01)

4.5.2 Effect of Celecoxib in T-cell Suppression Assays

The additon of a non-toxic concentration of Celecoxib (2.5μM) was studied in several suppression assays, in the presence of $CD11b^{+}CD33^{+}$ cells, obtained from co-cultures of PBMCs and different tumor cell lines. For suppression assays seeded in a 4:1 ratio, no differences in T-cell proliferation were found, when compared to the correspondent conditions in the absence of Celecoxib. No differences in T-cell proliferation were either observed when comparing several settings to the correspondent conditions, in the absence of Celecoxib, in 8:1 seeding ratios [p> 0.05] (Figure 18).

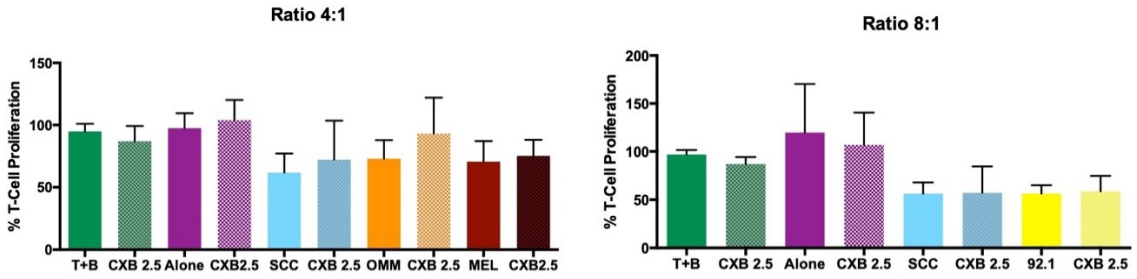

Figure 18: Percentage of T-cell proliferation in suppression assays with myeloid cells from PBMCs cultured alone and PBMCs cultured with tumor cells, in 2 different seeding ratios. Data presented as percentage of T-cell proliferation, in reference to T-cells cultured with Dynabeads™ (data from at least 3 different donors; mean ± SD). Differences in percentage analyzed by ANOVA and Tukey's multiple comparison test, for comparison of pairs of conditions with and without Celecoxib 2.5μM.

4.6 Cytokine production in PBMCs/ tumor cells co-cultures

Production of cytokines was evaluated by a 14-plex analysis of supernatants from PBMCs/ tumor cells co-cultures. Statistical significant differences in the concentration of GM-CSF, IFN-γ, IL-1β, IL-6, IL-10 and TNF-α were found among the cell lines tested. Considering GM-CSF, concentration of this growth factor was significantly higher in co-cultures with SCCL-MT1 (t=6,36; p<0.001) and 92.1 (t=3,57; p=0.013) cell lines, when compared to cultures of PBMCs in the absence of tumor cells. Concentrations of GM-CSF found in the supernatants of PBMCs/

SCCL-MT1 co-cultures were significantlly higher compared to co-cultures of PBMCs and UM cell lines MEL270 (t=3,97; p=0.005) and OMM2.5 (t=4,10; p=0.004).

The concentration of IFN-γ was significantly higher in co-cultures with UM cell lines MEL270 (t=5,8; p<0.001), OMM2.5 (t=4,66; p=0.001) and 92.1 (t=5,11; p<0.001), when compared to cultures of PBMCs in the absence of tumor cells. Concentrations of IFN-γ found in the supernatants of PBMCs/ SCCL-MT1 co-cultures were significantlly lower compared to co-cultures of PBMCs with UM cell lines OMM2.5 (t=-3,5; p=0.016) and 92.1 (t=3,62; p=0.012).

For IL-1β, concentration of this cytokine was significantly higher in co-cultures with tumor cell lines SCCL-MT1 (t=3,52; p=0.012), MEL270 (t=2,95; p=0.045) and OMM2.5 (t=3,13; p=0.031), when compared to cultures of PBMCs in the absence of tumor cells. Concentrations of the pro-inflammatory cytokine IL-6, was significantly higher in co-cultures with tumor cell lines SCCL-MT1 (t=7,28; p<0.001), MEL270 (t=8,72; p<0.001), OMM2.5 (t=8,68; p<0.001) and 92.1 (t=7,79; p<0.001), when compared to cultures of PBMCs in the absence of tumor cells.

Considering IL-10, concentration of this cytokine was significantly higher in co-cultures with tumor cell lines SCCL-MT1 (t=5,20; p<0.001), MEL270 (t=3,45; p=0.017), OMM2.5 (t=4,58; p=0.001) and 92.1 (t=4,44; p=0.002), when compared to cultures of PBMCs in the absence of tumors. Finally, concentration of TNF-α was significantly lower in co-cultures with tumor cell lines SCCL-MT1 (t=-5,03; p<0.001) and MEL270 (t=-3,26; p=0.023), when compared to cultures of PBMCs in the absence of tumor cells. Concentrations of this cytokine found in the supernatants of PBMCs/ SCCL-MT1 co-cultures were significantly lower compared to co-cultures of PBMCs and UM cell line 92.1 (t=4,65; p=0.001). A significant difference was also found in the concentration of TNF-α between co-cultures of PBMCs with MEL270 and 92.1, being higher in the latter (t=3.38; p=0.017).

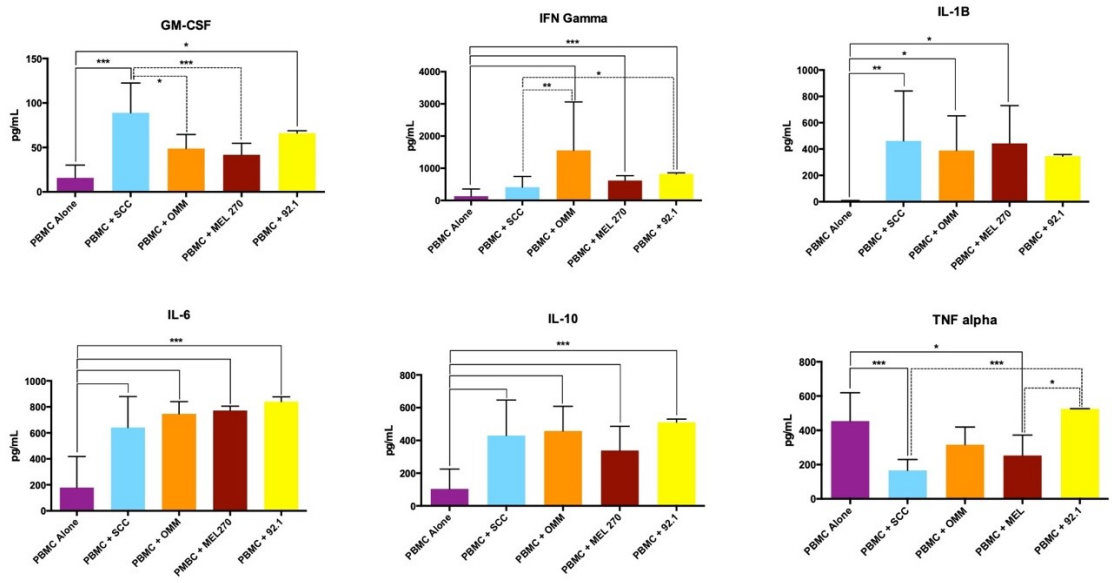

Figure 19: Concentration of growth factors/ cytokines in the supernatants of PBMCS alone and PBMCs/ tumor cells co-cultures (data from at least 3 different donors; mean ± SD). Differences in percentage analyzed by ANOVA and Tukey's multiple comparison test. (*, ** and *** indicate statistical significant differences in mean percentage between 2 groups; *p<0.05, ** p<0.01, ***p<0.001)

To complement these experiments, we conducted one induction assay in which we plated, in parallel, the same number of tumor cell lines alone, and analyzed supernatants for the same cytokines. Considering GM-CSF, the concentration of this growth factor was almost insignificant in all tumor cell lines supernatants, except SCCL-MT1, in comparison to co-cultures with tumor cells [$F(8,18)= 5655.22$; $p<0.001$]. The concentration of IFN-γ [$F(8,18)= 946.36$; $p<0.001$], IL-1β [$F(8,18)= 96.23$; $p<0.001$], IL-6 [$F(8,18)= 996.36$; $p<0.001$] and IL-10 [$F(8,18)= 1398.85$; $p<0.001$] was significantly lower in cultures of tumor cell lines, comparing to co-cultures of PBMCs and tumor cells supernatants. Finally, TNF-α showed high concentrations in the supernatant of PBMCs cultured alone, which were significantly higher than co-cultures of PBMCs with tumor cells, which in turn, also contrasted with residual concentrations of this cytokine in tumor cell line cultures [$F(8,18)= 775.71$; $p<0.001$].

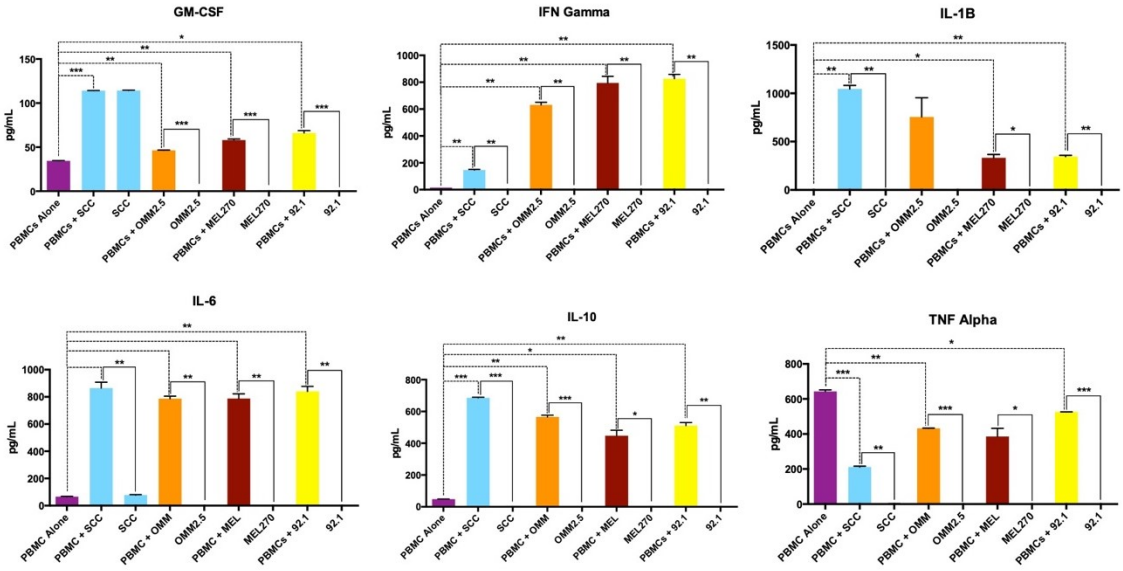

Figure 20: Concentration of growth factors/ cytokines in the supernatants of PBMCS alone, tumor cells alone and PBMCs/ tumor cells co-cultures (data from one experiment with triplicates for each condition; mean ± SD). Differences in percentage analyzed by ANOVA and Tukey's multiple comparison test. (*, ** and *** indicate statistical significant differences in mean percentage between 2 groups; *p<0.05, ** p<0.01, ***p<0.001)

4.6.2 Exploratory analysis of the effect of co-culture cytokines on T-cell proliferation

We aimed to explore whether cytokine concentrations in the supernatants could predict subsequent T-cell proliferation on suppression assays. Cytokines/growth factors that showed statistically significant differences among the cell lines tested were considered for analysis. For each cytokine, a univariate linear regression model was built. Supernatant concentrations of IL-6 and TNF-α were considered predictors of T-cell proliferation. For each 100 pg/mL increase in IL-6 concentration, T-cell proliferation decreased by 5%, and for each 100 pg/mL increase in TNF-α concentration, T-cell proliferation increased by 7%.

Table 2. Univariate Analysis of T-cell proliferation		
Cytokines/ Growth factors	**β-coefficient (95% CI)**	**p-value***
GM-CSF	-0.35 (-0.70; 0.01)	0.054
IFN-γ	-0.03 (-0.06; 0.002)	0.072
IL-1β	-0.02 (-0.05; 0.009)	0.157
IL-6	-0.05 (0.08; -0.02)	**0.002***
IL-10	-0.04 (-0.09;0.007)	0.091
TNF-α	0.07 (0.02-0.13)	**0.006***

Table 2: Univariate Analysis of T-cell proliferation and cytokines/ growth factors concentration
CI: Confidence interval; *p<0.05

5. DISCUSSION

MDSCs are a diverse population of cells that integrate the TME, being responsible for complex interactions between the immune system and tumors. In the present study, we defined a methodology for *in vitro* generation of $CD11b^+CD33^+$ myeloid cells from healthy donors, in a 5-days period, in significant quantities for further functional studies. Using this method, we evaluated several UM cell lines for the ability to induce human $CD11b^+CD33^+$ myeloid cells and studied their suppressive abilities.

5.1 Phenotypic characterization of induced $CD11b^+CD33^+$ cells

The phenotypes of $CD11b^+CD33^+$ myeloid cells isolated from co-cultures of PBMCs in the presence and absence of tumor cell lines were evaluated regarding surface markers established for MDSCs. In humans, MDSCs can be distinguished from neutrophils and monocytes based on phenotypic markers and density gradient separation. In peripheral blood, MDSCs are found in PBMCs after Ficoll gradient separation. PMN-MDSCs and neutrophils share a similar phenotype $CD11b^+CD33^+CD14^-CD15^+$ (or $CD66b^+$), but density gradient separation segregates them in the low-density and high-density fractions, respectively [46,51,81]. Monocytes and M-MDSCs can be separated based on the expression of MHC class II molecules, the latter being HLA-$DR^{-/low}$ [46,51,81].

Our results show that isolated $CD11b^+CD33^+$ cells from co-cultures with tumor cell lines decreased the intensity of $CD11b^+$ expression and, more importantly, HLA-DR (except for MP-41), in comparison to PBMCs cultured in the absence of tumor cells. Therefore, this study corroborates CD11b and CD33 as markers of human MDSCs and, a decrease in the expression of HLA-DR, as an important characteristic of myeloid suppressive cells. Changes in myeloid cells phenotype are consistent among PBMCs cultured in the presence of tumor cells (except

MP41), in comparison with the phenotype displayed by PBMCs cultured in the absence of tumor cells. Phenotype changes occur, at least, within 5 days of co-culture without cell-to-cell contact.

5.2 Functional characterization of induced $CD11b^+CD33^+$ cells

T-cell proliferation in the presence of $CD11b^+CD33^+$ myeloid cells was evaluated at different ratios and compared to proliferation controls. T-cells, when combined with serial dilutions of $CD11b^+CD33^+$ cells, isolated from cultures of PBMCs alone, showed increasing proliferation percentages. This observation showed that, not only $CD11b^+CD33^+$ obtained from PBMCs cultured in the absence of tumor cells did not interfere with T-cell proliferation, but also stimulated it, at higher co-culture ratios.

In contrast, T-cell proliferation was significantly decreased for all myeloid cell dilutions, when those cells were obtained from co-cultures with head and neck tumor cells (SCCL-MT1). These results show that $CD11b^+CD33^+$ myeloid cells induced by SCCL-MT1 cells are able to suppress T-cell proliferation, even when their counts are significantly outnumbered. In previous publications, Leschner M *et al* extensively described the ability of this tumor cell line to generate potent suppressive $CD33^+$ MDSCs, capable of blocking both T-cell proliferation and IFN-γ production [77]. These authors determined that human $CD33^+$ MDSCs induced by SCCL-MT1 cell line mediated suppression by up-regulation of canonical suppressive mechanisms (iNOS and NOX-2) [77].

Serial dilutions of myeloid cells, isolated from PBMCs cultured in the presence of UM cell lines, also significantly decreased T-cell proliferation. For primary UM cell lines, both MEL270 and 92.1 cell lines were able to induce the generation of $CD11b^+CD33^+$ cells, that showed significant suppressive abilities towards $CD3^+$ cells, in serial dilution ratios. However, this was

not observed for MP41 UM cell line. UM OMM2.5 cell line, derived from a metastatic site, also presented the ability to induce $CD11b^{+}CD33^{+}$ myeloid cells, capable of halting T-cell proliferation, in serial dilutions. These observations demonstrate that UM primary and metastatic cell lines have the ability to induce suppressive MDSCs, which retain their suppressive abilities even when largely diluted, similarly to what would happen *in vivo*.

Comparisons between T-cell proliferation percentages among different induction tumor cell lines, showed different suppressive potencies of $CD11b^{+}CD33^{+}$ cells. At lower dilution ratios, all the tumor cell lines tested were able to induce $CD11b^{+}CD33^{+}$ myeloid cells that significantly decreased T-cell proliferation. However, with increasing dilutions, only SCCL-MT1 and UM 92.1-induced myeloid cells, retained significant suppressive abilities. Leschner M *et al* evaluated the ability of over 100 human solid tumor cell lines to induce human MDSCs from healthy donor PBMCs, and found that those suppressor cells could be generated from a wide variety of cancers [77]. Furthermore, these authors reported a range of suppressive ability within histologic types for the majority of cell lines examined, suggesting that specific cell subpopulations, within the whole heterogeneous tumor, may drive MDSC induction [77]. In cancer, cellular heterogeneity and phenotypic plasticity are key features underlying disease progression and resistance to therapy, and UM is no exception [82]. A recent multidimensional platform analysis defined four molecular UM subsets, which differed in their genetic aberrations, genomic copy number variations (CNVs), methylation profiles, GEP, metabolomic and immunological characteristics [6,24]. In the TCGA study, poor prognosis M3-UM shared a global DNA methylation pattern, but were subdivided in two clusters with distinct biological pathway profiles. Particularly, in terms of immune infiltration and regulation, differential gene expression analysis revealed that poor prognosis cluster 4 UMs were enriched for immune genes, such as genes involved in IFN-γ signaling, T-cell invasion (CXCL9 and CXCL13),

cytotoxicity and immunossupression (IDO1, TIGIT, IL6, IL10 and FOXP3) [24]. Recent findings from single-cell RNA (scRNA) sequencing analysis of primary and metastatic UM samples revealed a complex tumor and immune microenvironment that suggest co-evolution of both tumor and immune populations [83]. This study showed clonally expanded T-cells and/or plasma cells in UM samples, indicating that tumor infiltrating immune cells contribute to an immunossupressive environment [83]. Based on the aforementioned, and considering that tumor cell lines are a limited representation of the vast heterogeneity and complexity of a *in vivo* cancer, we hypothesize that the variability observed in MDSC-induction properties among distict UM cell lines, reflects the genetically and phenotypically heterogeneous cell populations, that constitute human cancers.

5.3 Influence of Celecoxib in the suppressive activity of induced $CD11b^+CD33^+$ cells

The addition of Celecoxib to suppression assays aimed to evaluate the potencial of a selective COX-2 inhibitor to rescue T-cell proliferation, in the presence of $CD11b^+CD33^+$ myeloid cells. However, our results did not show significant and consistent results with any of Celecoxib concentrations, in any of the culture ratios tested. We mainly focused our experiments in the 2.5 μM concentration based on the rationale of possible interference of higher concentrations with T-cell proliferation, as observed in the T-cell proliferation control with Celecoxib 10 μM. However, no significant effect on T-cell proliferation was observed with the addition of Celecoxib 2.5 μM, in all suppression assays assembled.

Inflammatory mediator PGE_2, a lipid prostanoid, is produced in a COX-2 dependent pathway, by tumor stromal cells, tumor infiltrating leukocytes and tumor cells [66]. COX-2/PGE_2 were shown to play an important role in the activation and expansion of MDSCs. Blidner AD *et al* showed that indomethacin (a nonsteroidal anti-inflammatory, anti COX-1/2

drug) could influence the activity of MDSCs depending on the context they were derived from (TME or tumor-free microenvironment - TFME) [84]. When progenitor hematopoietic cells were cultured in a TFME with GM-CSF supplementation, the presence of indomethacin was associated with a robust suppressive function of *in vitro* induced MDSCs. In contrast, when those cells were cultured with GM-CSF supplementation and LP07 (lung adenocarcinoma cell line) conditioned medium, mimicking TME, the suppressive activity of these cells was abolished by the introduction of indomethacin [84]. This study shows the positive effect of a nonsteroidal anti-inflammatory drug on MDSC supressive activity and, the relevance of TME in the induction and activation of MDSCs [84]. In our research setting, this crosstalk would be established during the co-cultures between tumor cells and PBMCs, thus possibly explaining the lack of effect of Celecoxib on T-cell proliferation, when introduced in subsequent suppression assays.

5.4 Cytokine production in PBMC/ tumor cells co-cultures

According to the setup of our assays, co-cultures of PBMCs and tumor cells were physically separated by a a 0.4 μm pore transwell insert to prevent cell-to-cell interaction. After 5 days, $CD11b^{+}CD33^{+}$ cells were isolated from PBMCs and our results show that these cells acquired phenotypic and funtional features of MDSCs. These data suggest that many, if not all MDSC induction and expansion mechanisms, are mediated by soluble factors.

Growth factor and cytokine production were evaluated by measurement of protein concentrations in the supernatants of PBMCs/ tumor cells co-cultures. Significant differences in the concentrations of GM-CSF, IFN-γ, IL-1β, IL-6, IL-10 and TNF-α were found, which is in accordance to numerous studies in the literature [46,47,53,54,55,57].

Leschner M *et al* evaluated cytokine mixtures to generate *in vitro* human MDSCs from healthy donor PBMCs [57]. These authors showed generation of very potent suppressive $CD33^+$ MDSCs after incubation of PBMCs with GM-CSF + IL-6 and GM-CSF + IL-6 + VEGF. Similarly, incubation of PBMCs in the presence of GM-CSF, GM-CSF + IL-1β, GM-CSF + TNF-α and GM-CSF + VEGF also induced MDSCs with significant suppressive activity. These data suggested an important role for IL-1β, IL-6, TNF-α, GM-CSF and VEGF in MDSCs induction [57].

Comparably, our work showed significantly higher concentrations of GM-CSF in supernatants obtained from co-cultures of PBMCs with SCCL-MT1 and 92.1 cell lines, which corresponded to tumor cell lines associated with generation of $CD11b^+CD33^+$ cells with significant suppressive abilities. However, our exploratory analysis did not find GM-CSF concentration to be predictive of T-cell proliferation, which may be related to a small absolute number of observations, limiting the power of this analysis.

Moreover, the concentration of GM-CSF was the highest for co-cultures of PBMCs and SCCL-MT1 in comparison to UM cell lines, with significant difference from MEL270 and OMM2.5. Leschner M *et al* showed that GM-CSF was barely expressed by MDSC-inducing tumor cell lines and PBMCs cultured in medium only, in contrast with PBMCs cultured in the presence of MDSCs-inducing tumor cell lines (SCCL-MT1 included), where it was significantly expressed [57]. This study suggested that GM-CSF would be produced by PBMCs in the TME, in response to tumor cell contact [57]. In contrast, our analysis of tumor cell lines supernatants showed high concentrations of GM-CSF in SCCL-MT1 cell cultures, in opposition to the supernatants of all UM cell lines.

Focusing on IL-1β and IL-6, we observed that concentrations of these cytokines were significantly increased in supernatants obtained from co-cultures for almost all tumor cell lines, in comparison to PBMCs cultured alone and tumor cell lines alone. As described by

Leschner M *et al,* combination of IL-6 and GM-CSF generated the most suppressive $CD33^+$ cells, measured by T-cell proliferation and IFN-γ production assays [57]. Those suppressive MDSCs exerted their function through up-regulation of ARG-1, iNOS, VEGF and TGF-β. As for IL-1β, this cytokine has been described to be produced by the inflammatory TME and activate MDSCs through the NF-κB and STATA1 pathways [50,52,54].

Our data demonstrated significantly higher concentrations of IL-10 in co-cultures with tumor cells, in comparison to PBMCs cultured in medium only and tumor cell lines alone. MDSCs are a major source of IL-10 and the frequency of these cells in tumor bearing hosts correlates with levels of IL-10 in the bloodstream [74]. This cytokine plays an important role in the suppressive activity of MDSCs, which is supported by observations that blockade of IL-10 signaling eased T-cell suppression, slowed tumor progression and improved therapeutic efficacy [52,74]. We hypothesize that higher concentrations observed in co-cultures with tumor cells reflect induction of MDSCs, and consequent production of IL-10.

Our experiment showed a decrease in the production of TNF-α in co-cultures of PBMCs with SCCL-MT1 and MEL270, when compared to PBMCs cultured alone. In contrast, co-cultures of PBMCs with OMM2.5 and 92.1 cells did not show significant differences in the concentration of TNF-α in the supernatants, in comparison to PBMCs in the absence of tumor cells and tumor cell lines alone. TNF-α plays a role in anti-tumor activity, immune modulation, inflammation, viral replication, systemic infections and hematopoiesis. It is produced by a great variety of cells, but primarly activated macrophages, T-lymphocytes and NK cells [85]. Our results confirm that this cytokine is produced by populations in the PBMCs, and we hypothesize that the decrease of TNF-α production may reflect the immunossupressive effect of induced MDSCs in co-cultures.

6. CONCLUSIONS

This project developed a valid methodology for *in vitro* generation of MDSCs from healthy donors PBMCs, in a short time period. These cells were generated in significant quantities to allow further studies. Our method demonstrated that induction of MDSCs was cell-to-cell independent and achieved by soluble factors, in a crosstalk that occurs in the TME. The analysis of supernatants collected from PBMCs/ tumor cells co-cultures confirmed that growth factors and inflammatory cytokines such as GM-CSF, IL-1β and IL-6 may play an important role in MDSCs induction and expansion.

Isolated myeloid cells displayed consistent CD11b, CD33 and HLA-DR^{low} surface expression, established phenotypic markers of human MDSCs. Furthermore, *in vitro* UM-induced MDSCs exhibited suppressive properties and were able to decrease autologous T-cell proliferation. Both UM primary and metastatic cell lines showed the ability to induce suppressive MDSCs from PBMCs, with different suppressive potencies. However, the addition of Celecoxib was not effective in rescuing T-cell proliferation.

Future studies should explore possible genomic/ transcriptomic factors, that may explain distinct suppressive potencies in UM cell lines, in an attempt to further understand UM heterogeneity. Also, future research perspectives should focus on the role of soluble factors in MDSC induction, in a search for possible therapeutic targets. Finally, research pathways such as the role of COX-2 inhibitors, introduced as a possible modulator of the TME in MDSC induction, should be pursued.

In conclusion, the mechanisms regulating UM immune escape remain elusive and are partially responsible for its progressive course, poor prognosis and treatment resistance. Significant gaps in the current knowledge have to be filled before therapies directed at MDSCs can be translated into clinical research. The present project contributes to a better

understanding of the innate immune system in UM and paves the way for further research in this fascinating topic.

7. REFERENCES

1. Kranz BA, Dave N, Komatsubara KM *et al. Uveal melanoma: epidemiology, etiology, and treatment of primary disease*. Clinical Ophthalmology. 2017; 11:279–289
2. Kaliki S, Shields CL. *Uveal melanoma: relatively rare but deadly cancer*. Eye. 2016; 1–17
3. Virgili G, Gatta G, Ciccolallo L *et al. Incidence of Uveal Melanoma in Europe.* Ophthalmology 2007; 114: 2309-2315
4. Singh AD, Turell ME, Topham AK. *Uveal Melanoma: Trends in Incidence, Treatment, and Survival.* Ophthalmology 2011. 118: 1881-1885
5. Ghazawi FM, Darwich R, Le M *et al*. *Uveal melanoma incidence trends in Canada: a national comprehensive population-based study*. Br J Ophthalmol 2019. 103: 1872-1876
6. Jager M, Shields CL, Cebulla CM *et al*. *Uveal Melanoma*. Nat Rev Dis Primers. 2020. Apr 9 ; 6(1) :24
7. Amaro A, Gangemi R, Piaggio F *et al*. *The biology of uveal melanoma.* Cancer Metastasis Rev 2017. 36: 109-140
8. Andreoli MT, Mieler WF, Leiderman YI. *Epidemiological trends in uveal melanoma*. Br J Ophthalmol 2015. 99: 1550-1553
9. Eagle RC. *Eye Pathology – An Atlas and Text*. 3rd Edition. 2017. Wolters Kluwer; 539-573
10. McLean IW, Saraiva VS, Burnier MN, Jr. *Pathological and prognostic features of uveal melanomas*. Can J Ophthalmol 2004. 39 (4):343-350.
11. Damato B. *Progress in the management of patients with uveal melanoma*. *The 2012 Ashton Lecture*. Eye 2012. 26: 1157–1172
12. Spencer WH. Ophthalmic Pathology: an Atlas and Textbook. 4th Edition. Philadelphia: W.B. Saunders. 1996.

13. McLean IW, Foster WD, Zimmerman LE *et al*. *Modifications of Callender's classification of uveal melanoma at the Armed Forces Institute of Pathology*. Am J Ophthalmol. 1983. 96(4): 502-509.
14. Shields JA, Shields CL. *Management of Posterior Uveal Melanoma: Past, Present, and Future. The 2014 Charles L. Schepens Lecture*. Ophthalmology 2015. 122: 414-428
15. Margo CE. *The Collaborative Ocular Melanoma Study: An Overview*. Cancer Control 2004. 11(5): 304-309
16. Collaborative Ocular Melanoma Study Group. *The COMS randomized trial of iodine 125 brachytherapy for choroidal melanoma, V: Twelve-year mortality rates and prognostic factors. COMS Report no. 28*. Arch Ophthalmol 2006. 124: 1684-1693
17. Collaborative Ocular Melanoma Study Group. *The COMS randomized trial of iodine 125 brachytherapy for choroidal melanoma, III: Initial Mortality Findings. COMS Report no. 18*. Arch Ophthalmol 1998. 125(6): 779-796
18. Yang J, Manson DK, Marr BP, *et al. Treatment of uveal melanoma: where are we now?* Ther Adv Med Oncol. 2018. 10: 1-17
19. Kivelä T, Simpson RE, Grossniklaus HE, *et al. Uveal melanoma. AJCC Cancer Staging Manual*. 8th ed. New York, NY: Springer; 2016: 805-817
20. Kaliki S, Shields C, Shields JA. *Uveal melanoma: Estimating prognosis*. Indian J Ophthalmol 2015. 63; 93-102
21. Frizziero L, Midena E, Trainiti S *et al*. *Uveal Melanoma Biospy: A Review*. Cancers. 2019; 11: 1075
22. Onken MD, Worley LA; Char DH *et al*. *Collaborative Ocular Oncology Group report number 1: Prospective validation of a multi-gene prognostic assay in uveal melanoma.* Ophthalmology 2012. 119: 1596–1603

23. Robertson AG, Shih J, Yau C *et al*. *Integrative Analysis Identifies Four Molecular and Clinical Subsets in Uveal Melanoma.* Cancer Cell 2017. 32: 204-220
24. Bakhoum MF, Esmaeli B. *Molecular Characteristics of Uveal Melanoma: Insights from the Cancer Genome Atlas (TCGA) Project*. Cancers 2019. 11: 1061
25. Carvajal RD, Schwartz GK, Tezel T *et al*. *Metastatic disease from uveal melanoma: treatment options and future prospects*. Br J Ophthalmol 2017. 101(1): 38–44
26. Sacco JJ, Kalirai H, Kenyani J, *et al. Recent breakthrough in metastatic uveal melanoma: a cause for optimism?* Future Oncol. 2018. 14(14): 1335-1338
27. Vishal J. *Role of immune checkpoint inhibitors and novel immunotherapies in uveal melanoma.* Chin Clin Oncol 2018. 7(1):8
28. Chen DS, Mellman I. *Elements of cancer immunity and the cancer–immune set point*. Nature 2017. 541: 321-330
29. Hanahan D, Weinberg RA. *Hallmarks of Cancer: The Next Generation.* Cell 2011. 144 (4): 646-674
30. Basile MS, Mazzon E, Fagone P *et al*. *Immunobiology of Uveal Melanoma: State of the Art and Therapeutic Targets*. Front Oncol. 2019. 9:1145
31. Hanahan D, Weinberg RA. *Hallmarks of Cancer.* Cell 2000. 100(1): 57-70
32. Zitvogel L, Apetoh L, Ghiringhelli F *et al*. *The anticancer immune response: indispensable for therapeutic success?* The Journal of Clinical Investigation 2008. 118(6): 1991-2001
33. Nichols, EE, Richmond A, Daniels AB. *Micrometastatic Dormancy in Uveal Melanoma: A Comprehensive Review of the Evidence, Mechanisms, and Implications for Future Adjuvant Therapies*. International Ophthalmology Clinics 2017. 57(1): 1-10
34. Blanco PL, Lim LA *et al*. *Uveal melanoma dormancy: an acceptable clinical endpoint?* Melanoma Research. 2012; 22:334–340

35. Leone K, Poggiana C, Zamarchi R. BA, Dave N, Komatsubara KM *et al. The Interplay between Circulating Tumor Cells and the Immune System: From Immune Escape to Cancer Immunotherapy*. Diagnostics 2018; 8 (59): 1-46
36. Kim R, Emi M, Tanabe K. *Cancer immunoediting from immune surveillance to immune escape.* Immunology 2007. 121: 1-14
37. Teng ML, Swann JB, Koebel CM *et al. Immune-mediated dormancy: an equilibrium with cancer.* J Leukoc Biol 2008. 84: 988-993
38. Bronkhorst IHG, Jager MJ. *Uveal Melanoma: The Inflammatory Microenvironment*. J Innate Immun 2012. 4:454–462
39. Bronkhorst IHG, Jager MJ. *Inflammation in uveal melanoma*. Eye 2013. 27: 217-223
40. Keino H, Horie S, Sugita S. *Immune Privilege and Eye-Derived T-Regulatory Cells.* J Immunol Research 2018. ID 1679197
41. Rossi E, Schinzari G, Zizzari IG *et al. Immunological Backbone of Uveal Melanoma: Is There a Rationale for Immunotherapy?* Cancers 2019. 11: 1055
42. Eskelin S, Pyrhonen S, Summanen P, *et al*. *Tumor doubling times in metastatic malignant melanoma of the uvea. Tumor progression before and after treatment.* Ophthalmology. 2000; 107: 1443–1449
43. Singh A. *Uveal melanoma: implications of tumor doubling time.* Letter to the editor. Ophthalmology. 2000; 107: 829
44. Callejo SA, Antecka E *et al. Identification of circulating malignant cells and its correlation with prognostic factors and treatment in uveal melanoma: A prospective longitudinal study*. Eye. 2007; 21: 752–759

45. McKenna KC, Kapp JA. KM. *Accumulation of Immunossupressive CD11b^{+} myeloid cells correlates with the failure to prevent tumor growth in the anterior chamber of the eye.* Journal of Immunology 2006. 177: 1599-1608
46. Gabrilovich DI. *Myeloid-derived suppressor cells.* Cancer Immunol Res 2017. 5(1): 3–8
47. Gabrilovich D, Ostrand-Rosenberg S, Bronte V. *Coordinated regulation of myeloid cells by tumours.* Nature Reviews 2012. 12: 253-268
48. Vetsika E-K, Koukos A, Kotsakis A. *Myeloid-Derived Suppressor Cells: Major Figures that Shape the Immunosuppressive and Angiogenic Network in Cancer*. Cells 2019. 8; 1647
49. Talmadge JE, Gabrilovich DI. *History of myeloid-derived supressor cells*. Nature Reviews 2013. 13: 739-752
50. Jayakumar A, Bothwell ALM. *Cancer Suppressor Cells: The Multitasking Hydra of Functional Diversity of Myeloid-Derived*. J Immunol 2019. 203:1095-1103
51. Bronte V, Brandau S, Chen S-H *et al. Recommendations for myeloid-derived suppressor cell nomenclature and characterization standards.* Nature Communications 2016 Jul 6; 7:12150
52. Groth C, Hu X, Weber R *et al. Immunosuppression mediated by myeloid-derived suppressor cells (MDSCs) during tumour progression*. British Journal of Cancer 2019. 120:16–25
53. Nakamura K, Smyth MJ. *Myeloid immunosuppression and immune checkpoints in the tumo*r microenvironment. Cellular & Molecular Immunology 2020. 17(12): 1-12
54. Condamine T, Gabrilovich DI. *Molecular mechanisms regulating myeloid-derived suppressor cell differentiation and function.* Trends in Immunology 2011. 32(1): 19-25
55. Weber R, Fleming V, Hu *X et al. Myeloid-Derived Suppressor Cells Hinder the Anti-Cancer Activity of immune Checkpoint inhibitors.* Front. Immunol 2018. 9:1310

56. Umansky V, Blattner C, Gebhart C *et al*. *The Role of Myeloid-Derived Suppressor Cells (MDSC) in Cancer Progression*. Vaccines 2016. 4(36): 1-16

57. Lechner MG, Liebertz DJ, Epstein AL. *Characterization of cytokine-induced Myeloid-derived suppressor cells from normal human peripheral blood mononuclear cells.* J Immunol. 2010. 185(4): 2273–2284

58. Ostrand-Rosenberg S, Sinha P. *Inflammation and Cancer Myeloid-Derived Suppressor Cells: Linking Inflammation and Cancer.* J Immunol 2009. 182: 4499-4506;

59. Wang Y, Ding Y, Guo N *et al. MDSCs: Key Criminals of Tumor Pre-metastatic Niche Formation.* Front Immunol 2019. 10:172

60. Zhang S, Zhu C, Liu L *et al. The Role of Myeloid-Derived Suppressor Cells in Patients with Solid Tumors: A Meta-Analysis.* PLoS ONE 2016. 11(10): e0164514.

61. Ai L, Mu S, Wang Y *et al. Prognostic role of myeloid-derived suppressor cells in cancers: a systematic review and meta-analysis.* BMC Cancer 2018. 18: 1220

62. McKenna KC, Beatty KM, Bilonick RA *et al. Activated CD11b$^+$ CD15$^+$ Granulocytes Increase in the Blood of Patients with Uveal Melanoma.* IOVS 2009. 50(9): 4295-4303

63. Achberger S, Aldrich W, Tubbs R *et al. Circulating immune cell and microRNA in patients with uveal melanoma developing metastatic disease.* Mol Immunol. 2014. 58(2): 182–186

64. Liu B, Qu L, Yan S. *Cyclooxygenase-2 promotes tumor growth and suppresses tumor immunity.* Cancer Cell Int. 2015; 15:106

65. Goradel NH, Najafi M, Salehi E *et al. Cyclooxygenase-2 in cancer: A review.* J Cell Physiol 2019. 234: 5683-5699

66. Zelenay S, van der Veen AG, Bottcher JP *et al. Cyclooxygenase-Dependent Tumor Growth through Evasion of Immunity.* Cell 2015. 162: 1257-1270

67. Stasinopoulos I, Shah T, Penet MF *et al. COX- 2 in cancer: Gordian knot or Achilles heel?* Frontiers in Pharmacology 2013. 4(34): 1-7

68. Figueiredo A, Caissie AL, Callejo SA, *et al. Cyclooxygenase-2 expression in uveal melanoma: novel classification of mixed-cell-type tumours.* Can J Ophthalmol. 2003; 38(5): 352–356

69. Cryan LM, Paraoan L, Hiscott P, *et al. Expression of COX-2 and prognostic outcome in uveal melanoma.* Curr Eye Res. 2008; 33(2): 177–184

70. Marshall JC, Caissie AL, Cruess SR, *et al. The effects of a cyclooxygenase-2 (COX-2) expression and inhibition on human uveal melanoma cell proliferation and macrophage nitric oxide production*. J Carcinog. 2007; 6:17

71. Caissie AL. *Cyclooxygenase-2 and Other Targets of Adjuvant Therapies for Uveal Melanoma.* 2004. PhD Thesis. McGill University

72. Marshall JC, Fernandes BF, Di Cesare S *et al*. *The use of a cyclooxygenase-2 inhibitor (Nepafenac) in an ocular and metastatic animal model of uveal melanoma.* Carcinogenesis 2007. 28(9): 2053-2058

73. Sinha P, Clements VK, Fulton AM *et al*. *Prostaglandin E2 Promotes Tumor Progression by Inducing Myeloid-Derived Suppressor Cells.* Cancer Res 2007. 67(9): 4507-4513

74. Yang Y, Li C, Liu T *et al*. *Myeloid-Derived Suppressor Cells in Tumors: From Mechanisms to Antigen Specificity and Microenvironmental Regulation*. Front. Immunol 2020. 11(1371): 1-22

75. Rodriguez PC, Hernandez CP, Quiceno D *et al*. *Arginase I in myeloid suppressor cells is induced by COX-2 in lung carcinoma.* Journal Experimental Medicine 2005. 202(7): 931-939

76. Donkor MK, Lahue E, Hoke TA *et al. Mammary tumor heterogeneity in the expansion of myeloid-derived suppressor cells.* International Immunopharmacology 2009. 9: 937-948
77. Lechner M, Miegel C, Russell SM *et al. Functional characterization of human Cd33+ And Cd11b+ myeloid-derived suppressor cell subsets induced from peripheral blood mononuclear cells co-cultured with a diverse set of human tumor cell lines*. Journal of Translational Medicine. 2011; 9:90
78. Veltmand JD, Lambers MEH, van Nimwegen M *et al. COX-2 inhibition improves immunotherapy and is associated with decreased numbers of myeloid derived suppressor cells in mesothelioma. Celecoxib influences MDSC function*. BMC Cancer 2010, 10: 464
79. Obermajer N, Muthuswamy R, Lesnock J *et al*. *Positive feedback between PGE2 and COX2 redirects the differentiation of human dendritic cells toward stable myeloid-derived suppressor cells.* Blood 2011. 118(20): 5498-5505
80. Jager MJ, Magner JA, Ksander BR, Dubovy SR. *Uveal Melanoma Cell Lines: Where do they come from? (An American Ophthalmological Society Thesis).* Trans Am Ophthalmol Soc 2016; 114:T5
81. Veglia F, Perego M, Gabrilovich DI. *Myeloid-derived suppressor cells coming of age.* Nat Immunol 2018. 19(2): 108-119
82. Hinohara K, Polyak K. *Intratumoral Heterogeneity: More Than Just Mutations*. Trends in Cell Biology 2019. 29(7): 569-579
83. Durante MA, Rodriguez DA, Kurtenbach S *et al. Single-cell analysis reveals new evolutionary complexity in uveal melanoma.* Nature Communications 2020. 11(496): 1-10
84. Blidner AG, Salatino M, Mascanfroni ID *et al. Differential Response of Myeloid-Derived Suppressor Cells to the Nonsteroidal Anti-Inflammatory Agent Indomethacin in Tumor-*

Associated and Tumor-Free Microenvironments. Journal of Immunology 2015, 194: 3452–3462

85. Punt J, Stranford S, Jones P *et al*. *Kuby Immunology*. 8th Edition. 2018. WH Freeman